AD-A057 008 BOSTON UNIV MASS DEPT OF ASTRONOMY F/G 4/1
HIGH LATITUDE IONOSPHERIC GRADIENTS AND THEIR RELATIONSHIPS TO --ETC(U)
DEC 77 C C CHACKO, M MENDILLO F19628-75-C-0044
UNCLASSIFIED ACBU-SER-III-NO-4 AFGL-TR-78-0092(I) NL

1 OF 1
AD A057 008

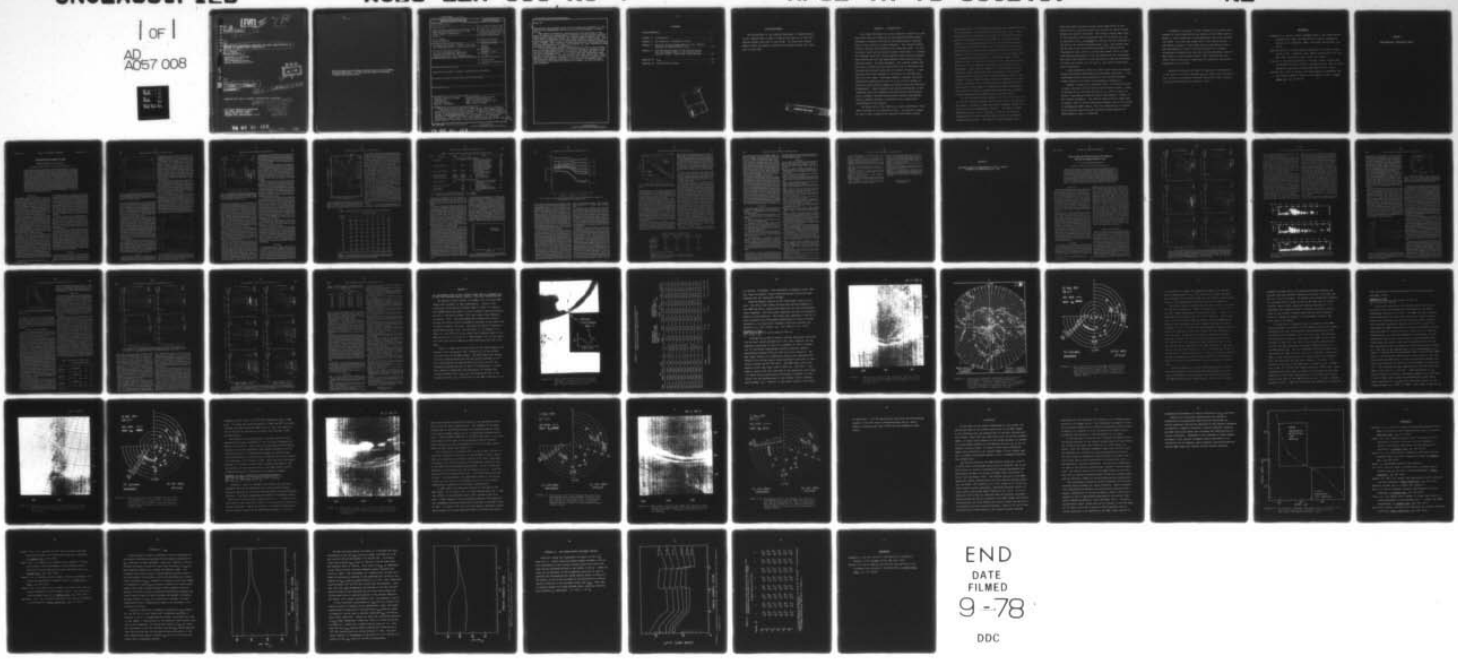

END
DATE FILMED
9-78
DDC

AD A057008

DDC FILE COPY

LEVEL III

(18) (19) AFGL-TR-78-0092(I)

See AD5-6978

(6) HIGH LATITUDE IONOSPHERIC GRADIENTS AND THEIR RELATIONSHIPS TO AURORAL AND MAGNETOSPHERIC BOUNDARIES.

(10) C. C. Chacko
Michael Mendillo

Department of Astronomy
Boston University
725 Commonwealth Avenue
Boston, Massachusetts 02215

DDC
RECEIVED
AUG 3 1978
F

(9) Final Scientific Report. Vol I
1 July 1975 - 31 Aug 1977,

(11) December 1977

(12) 63p.

(14) ACBU-SER-III-NO-4

Approved for public release; distribution unlimited.

(15) F19628-75-C-0044

(16) 4643

(17) 01

AIR FORCE GEOPHYSICS LABORATORY
AIR FORCE SYSTEMS COMMAND
UNITED STATES AIR FORCE
HANSCOM AFB, MASSACHUSETTS 01730

78 07 31 155

406 311 JOB

Qualified requestors may obtain additional copies from the Defense Documentation Center. All others should apply to the National Technical Information Service.

Unclassified

SECURITY CLASSIFICATION OF THIS PAGE (When Data Entered)

REPORT DOCUMENTATION PAGE		READ INSTRUCTIONS BEFORE COMPLETING FORM
1. REPORT NUMBER AFGL-TR-78-0092(I)	2. GOVT ACCESSION NO.	3. RECIPIENT'S CATALOG NUMBER
4. TITLE (and Subtitle) High Latitude Ionospheric Gradients and Their Relationships to Auroral and Magnetospheric Boundaries		5. TYPE OF REPORT & PERIOD COVERED Scientific - Final Vol. I 1 July 1975-30 Sept 1977 6. PERFORMING ORG. REPORT NUMBER A.C.B.U., SerIII, no. 4
7. AUTHOR(s) C. C. Chacko Michael Mendillo		8. CONTRACT OR GRANT NUMBER(s) F-19628-75-C-0044
9. PERFORMING ORGANIZATION NAME AND ADDRESS Astronomy Department, Boston University 725 Commonwealth Ave., Boston, MA 02215		10. PROGRAM ELEMENT, PROJECT, TASK AREA & WORK UNIT NUMBERS 62101F 46430107
11. CONTROLLING OFFICE NAME AND ADDRESS Air Force Geophysics Laboratory Hanscom AFB, Bedford, MA 01731 Contract Monitor: J.A. Klobuchar/PHP		12. REPORT DATE December, 1977 13. NUMBER OF PAGES 62
14. MONITORING AGENCY NAME & ADDRESS (if different from Controlling Office)		15. SECURITY CLASS. (of this report) Unclassified 15a. DECLASSIFICATION/DOWNGRADING SCHEDULE

16. DISTRIBUTION STATEMENT (of this Report)

Approved for public release; distribution unlimited

17. DISTRIBUTION STATEMENT (of the abstract entered in Block 20, if different from Report)

18. SUPPLEMENTARY NOTES

19. KEY WORDS (Continue on reverse side if necessary and identify by block number)

Electron Density Trough	Dayside Magnetospheric Cusp
Plasmapause	Particle Precipitations
Diffuse Aurora	ISIS 2 Electron Density Data
Auroral Ionosphere	DMSP Auroral Images

20. ABSTRACT (Continue on reverse side if necessary and identify by block number)

The main electron density trough in the topside ionosphere is investigated using ISIS 2 topside sounder data, DMSP auroral images and ground-based observations. A "base-level" ionospheric trough is characterized with the aid of ISIS 2 electron densities obtained in December 1971 under an optimum set of geophysical conditions, namely midwinter, local midnight and very quiet magnetospheric intervals. The statistical positions of the →

DD FORM 1 JAN 73 1473 EDITION OF 1 NOV 65 IS OBSOLETE

unclassified

SECURITY CLASSIFICATION OF THIS PAGE (When Data Entered)

78 07 31 155

Block 20

equatorward and poleward walls of the trough are examined in relation to the plasmapause and various auroral boundaries, respectively.

The effects created by precipitating soft particles in the upper F-region are investigated, focussing on the electron density enhancements observed beneath the dayside magnetospheric cusp near local noon in midwinter under very quiet magnetic conditions. The altitude dependence of the Cusp-Related Electron Density Enhancements (CREDE), their behavior during magnetically disturbed periods and the implications of these new findings for high latitude plasma convection models are discussed.

The relationship between the equatorward edge of the diffuse aurora and the poleward wall of the main trough is examined using ten near-simultaneous events recorded by the DMSP and ISIS 2 satellites in December 1971. It is found that the equatorward edge of the diffuse aurora (as monitored by the DMSP satellites) always appears a few degrees poleward of the main trough's poleward wall. The possible physical processes in the auroral ionosphere that could lead to the observed separation between the two boundaries are discussed.

CONTENTS

Acknowledgements v

Chapter 1. Introduction 1

Chapter 2. The Baselevel Ionospheric Trough 6

Chapter 3. Electron Density Enhancements in the F-Region Beneath the Magnetospheric Cusp 16

Chapter 4. The Equatorward Edge of the Diffuse Aurora and the Poleward Wall of the Main Electron Density Trough: Case Study Investigations 25

Appendix A: h_{max} 50

Appendix B: The Disturbed Trough 54

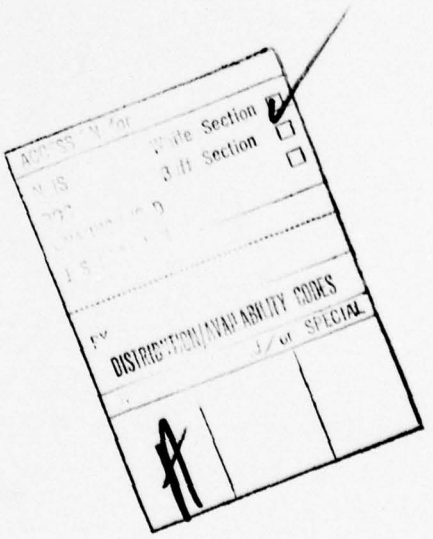

ACKNOWLEDGEMENTS

We are grateful to the Canadian Department of Communications and Dr. Charles Pike of AFGL for making available to us the ISIS 2 topside sounder data used in this study. We thank Capt. Edward Weber of AFGL for helpful scientific discussions during the latter part of this work.

PRECEDING PAGE BLANK

CHAPTER 1. INTRODUCTION

This report describes the final scientific results of a two-year study aimed at examining the relationship between severe ionospheric gradients and auroral and magnetospheric topology found in the vicinity of those gradients. Two F-region characteristic features were singled out for detailed study: (1) the so-called "main electron density trough" found near L = 4 during the nighttime hours and (2) the topside electron density enhancements associated with the magnetospheric cusp location in the noontime sector. For both phenomena, ISIS topside sounder data were used to define the most appropriate way of specifying the latitude and altitude variations in F-region structure. A substantial effort was expended in arriving at an "optimum data base" for each study. Stringent temporal, seasonal and solar-geophysical conditions were set up in an a priori attempt to define the best possible chances of finding clear and consistent morphologies. These optimized statistical descriptions of the ionosphere were then compared with appropriate auroral boundaries, energetic particle precipitation patterns and magnetospheric topology features to determine their quantitative relationships to one another.

The major part of the scientific results described in this report pertains to the nightside trough. The specific concept we wish to test concerned the detailed relationship between

the poleward wall of the F-region trough and the equatorward edge of the continuous (or diffuse) aurora (see Figure 4.1). Energetic particle precipitations are known to cause both features, and thus the question arises of whether or not detailed knowledge of the latitudinal pattern of one can be used to predict the detailed structure of the other. The notion of specifying optical auroral features from ionospheric data is not nearly as appealing as the reverse possibility, i.e., using a single optical photograph (obtained during a conventional DMSP or ISIS satellite pass) to specify the location of an important F-region structure over the extensive geographic area covered in the photograph. Since topside sounders or single-height, in-situ satellite probes provide the only routine way of specifying trough features (and only along a given satellite track), the concept of using satellite-borne "optical diagnostics" to infer F-region structure over a region much more extensive than the sub-satellite track implies a capability broadly equivalent to the unrealistic scheme of having many simultaneous ionospheric sounding satellites pass through a given world region.

In the following section (Chapter 2), the first step taken to test this "Auroral/Trough" scheme is described. An optimized data base is defined to study the winter nighttime trough for a period of very low geomagnetic activity. Following a scheme suggested by Pike (1976), the base or foot of the trough's poleward wall is used as the key anchor point for reckoning latitudinal structure. The concept is then expanded into a

multi-sectioned altitude/latitude trough model which is consistent with all previous statistical studies of various trough features at specific altitudes. The overall results imply that if the latitude of the equatorward edge of the aurora (ϕ_a) can be specified, and ϕ_a is assumed to coincide with the latitude of the base of the trough's poleward wall (ϕ_{pw}), this anchor point can be used to key the statistical models of Halcrow (1976), Feinblum and Horan (1973) or Rycroft and Thomas (1970) to real-time auroral photographs to give an estimate of the latitudinal and local time structure of the sub-auroral nighttime ionosphere to within an accuracy of $\simeq \pm 3^{o}$ near ϕ_a, for quiet to moderately active conditions.

A less exhaustive effort was given to the study of combined trough and auroral morphologies for disturbed conditions. A few significant results were obtained for the altitude/latitude trough structure, and these are presented in Appendix B.

Chapter 3 deals with a companion study of altitude/latitude F-region structure for the high latitude noontime sector. Again, an optimum set of data were defined in an a priori attempt to isolate "Cusp-Related Electron Density Enhancements" (CREDE) in the topside ionosphere. The results explain why the CREDE seem to exhibit such an elusive occurrence pattern, and in the process of documenting CREDE effects, the first detailed set of topside $N_e(h)$ profiles across the high latitude regions beneath the magnetospheric cusps is presented.

In Chapter 4, a series of "case studies" are described which examine in a real-time fashion the concept of using DMSP auroral images to infer ionospheric trough morphology over wide geographical areas. For each case study event, ISIS topside sounder latitudinal profiles of foF2 (made nearly simultaneously with a DMSP photograph) are used in conjunction with all available ground-based ionosonde data from the northern hemisphere and the AFGL chain of total electron content (TEC) observatories near 70^{o}W to make as detailed a comparison of ionospheric and auroral boundaries as is possible.

Appendix A addresses the specific question of the behavior of the height of F-region maximum (h_{max} or $h_{m}F2$) along the entire high latitude noon-midnight meridian, during the winter solstice low K_{p} periods described in Chapters 2 and 3.

REFERENCES

Feinblum, D.A. and R.J. Horan, HILION-A model of the high-latitude ionospheric F2 layer and statistics of regular ionospheric effects at Ft. Churchill, 1968. Bell Labs, Murray Hill, N.J. (1973).

Halcrow, Barry W., F2 peak electron densities in the main trough region of the ionosphere, Tech. Report PSU-IRL-IR-55 Ion. Res. Lab, Penn. State Univ., Univ. Park, PA, (1976).

Pike, C.P., An analytical model of the main F-layer trough, AFGL-TR-76-0098, Air Force Surveys in Geophysics, No. 348, Air Force Geophysics Laboratory, Hanscom AFB, Mass. 01731, (1976).

Rycroft, M.J. and J.O. Thomas, The magnetospheric plasmapause and the electron density trough at the Alouette I orbit, Planet. Space Sci., 18, 65 (1970).

CHAPTER 2

THE BASELEVEL IONOSPHERE TROUGH

VOL. 82, NO. 32 JOURNAL OF GEOPHYSICAL RESEARCH NOVEMBER 1, 1977

The Baselevel Ionospheric Trough

MICHAEL MENDILLO AND C. C. CHACKO

Department of Astronomy, Boston University, Boston, Massachusetts 02215

Isis 2 electron density profiles of the topside F region obtained during December 1971 have led to a detailed examination of the ionosphere's 'main trough' region under an optimum set of geophysical conditions. A total of 30 individual satellite passes during a 21-day period were used to determine the trough's characteristic features under the conditions of midwinter in the northern hemisphere, midnight local time, and very low magnetic activity. The morphological description obtained from this rigidly consistent data base is termed the 'baselevel trough.' The latitudinal profile of the trough at h_{max} over the 40°–80° corrected geomagnetic latitude range shows that while the equatorward edge and the trough minimum are wide features (7° and 10°, respectively), the poleward wall is sharp (~1½°). The equatorward edge and the trough minimum tend to lose their distinct identities toward higher altitudes, while the magnitude of the poleward wall enhancement remains nearly constant at 2.15 from 450 to 950 km. The trough's poleward wall is found 1°–2° lower in latitude than the statistical position of the equatorward edge of the diffuse aurora. Ratios of topside densities to the peak density reveal that the shape of the $N_e(h)$ profiles is constant from mid-latitudes to the trough minimum. Within the minimum a relatively rapid change in topside shape occurs which marks the light ion depletion region characterized by high H^+/O^+ transition heights. The northern terminus of the transition height enhancement agrees with the statistical position of the magnetospheric plasmapause. Estimates of plasma temperature ($T_e + T_i$) show only modest enhancements within the trough minimum.

INTRODUCTION

Since *Muldrew*'s [1965] initial description of the 'ionospheric trough' appeared, a wide variety of morphological studies have been carried out in attempts to understand more fully the trough's spatial and temporal variations. Discoveries of 'multiple troughs' and the 'light ion trough,' plus discussions of the trough's possible relationship to the plasmapause, added complexity to subsequent investigations of the trough. A certain amount of confusion and ambiguity continues to persist, the result being that the so-called 'main or mid-latitude' trough in F region electron densities is today an often used label for a still poorly understood phenomenon.

Satellite-borne probes [e.g., *Tulunay and Sayers*, 1971] and topside sounders [*Chan and Colin*, 1969; *Rycroft and Thomas*, 1970] have been the main data-gathering techniques for determining the trough's structure and behavior. These have been augmented at times by ground-based radio techniques [*Liszka*, 1965; *Evans and Holt*, 1973; *Bates et al.*, 1973; *G. N. Taylor*, 1973; *Mendillo and Klobuchar*, 1975] and magnetometer networks monitoring MHD wave polarization characteristics [*Lanzerotti and Fukunishi*, 1975; *Lanzerotti et al.*, 1976]. These methods offer, in effect, different views of the F region trough with varying amounts of latitudinal resolution.

In recent years there have been several attempts to unify large amounts of data into systematic specifications of the trough's characteristics [*Feinblum and Horan*, 1973; *Halcrow*, 1976; *Wildman et al.*, 1976]. The use of large data bases, spanning long periods of time and analyzed in statistical ways, provides a convenient way of examining overall trough effects. Yet in the very process of analyzing large amounts of data by using statistical techniques, distortions of latitudinal gradients are sometimes introduced. This can be particularly bothersome in seeking answers to questions involving the trough's specific relationship to such morphological features as the plasmapause, the auroral oval, the scintillation boundary, etc.

Perhaps the most intriguing aspect of trough morphology is the question of its relationship to the magnetospheric plasmapause. In *Thomas and Dufour*'s [1965] early study the feature of a 'troughed F region' was suggested to be the natural consequence of declining densities with latitude interrupted by aurorally produced ionization. Within this framework, however, it was not clear whether the foot of the field line marking the plasmapause fell along the equatorward edge of the trough or at its center. The studies of *Rycroft and Thomas* [1970] and *Rycroft and Burnell* [1970] showed, on a statistical basis, that the center of the trough minimum at 1000 km and the plasmapause measured in the equatorial plane were aligned along the same L shell. However, simultaneous observations of the trough and the plasmapause have recently raised questions about this relationship on a case-by-case basis [*Grebowsky et al.*, 1976].

In this paper, topside F region data are assembled for analysis of the trough under the very favorable conditions of a December solstice period, midnight local time, and very low geomagnetic activity. This optimum set of data is used to define what may be considered to be the 'baselevel trough.' The average morphology thus derived is expected to be more representative of individual troughs observed under comparable conditions.

In examining the literature on the F region trough we find that no uniform definitions have been applied to its characterization. We therefore start by reinvestigating the traditional procedures used for defining trough morphology. It also appears that very little attention has been given to examining whether or not parameters attributed to the trough (e.g., its position, width, or poleward wall gradient) depend upon the altitude sampled. This often neglected aspect of trough studies (only *Chan and Colin* [1969] describe it in any detail) could help interrelate previous statistical studies carried out for different heights, as well as contribute detailed vertical profile information to recent theoretical attempts to model the trough (see, for example, *Schunk et al.* [1976]).

DATA BASE

The data set used for this study was derived from the topside sounder measurements made by Isis 2 between December 6 and 27, 1971. The orbital configuration of the satellite during this period was such that the nightside mid-latitude portion of

Copyright © 1977 by the American Geophysical Union.

Paper number 7A0661.

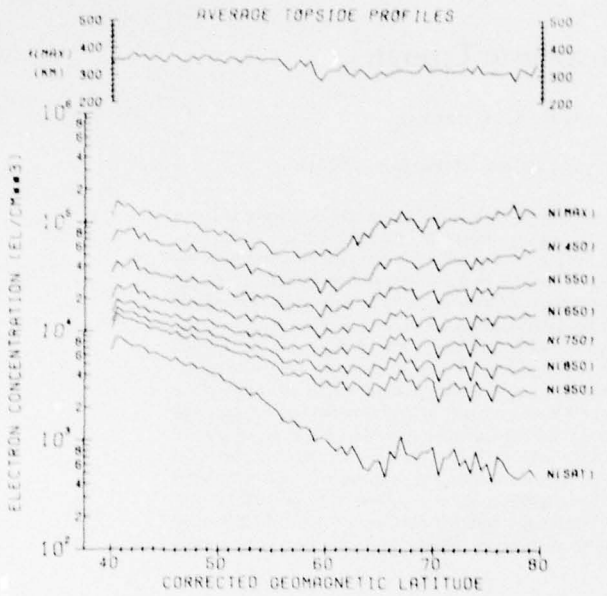

Fig. 1. Average electron densities in the 40°–80° CGL range at eight topside heights using data obtained from the topside sounder on Isis 2 between December 6 and 27, 1971. Thirty quiet time ($Kp \leq 1+$) passes near the midnight meridian (2230–2400 MLT) are used. The top panel shows average h_{max} behavior.

its track in the northern hemisphere was maintained within ½ hours of the midnight meridian. A remarkably large number (30) of the passes in this 21-day period spanning the winter solstice occurred during very quiet magnetospheric conditions ($Kp \leq 1+$). Of these 30 passes, four had large data gaps in the 40°–80° corrected geomagnetic latitude (CGL) range of interest to us. It was possible to identify a well-defined main trough (see the section on analysis) on 23 of the remaining passes, indicating an occurrence frequency of 88%.

A careful comparison with previous statistical studies shows that the above data set represents possibly the largest so far assembled for the midwinter quiet time trough near local midnight. *Tulunay and Savers* [1971] examined 1287 troughs, by far the largest absolute number of troughs included in a single statistical investigation. However, these data were collected over 11 months spanning all seasons, all local times, and the entire range of the Kp index. Included in this number were 43 winter (both hemispheres) troughs detected between 2200 and 2400 hours local time and ranging in Kp from 0o to 3+. Note that over one half of these passes would have had to occur in the middle of winter, during very quiet magnetic conditions ($Kp \leq 1+$) to equal the size of the data base adopted for the present study.

In our analysis, electron density values scaled from the lowest-quality ionograms were excluded. The data acquisition rate was high enough to afford, on the average, three electron density profiles for every 2° latitude. This is at least 50% better than the highest latitudinal resolution achieved previously [*Ryeroft and Thomas*, 1970]. The near-constant height of 1400 km maintained by the satellite also made it possible to examine the altitude dependence of the trough consistently.

Analysis

The first method we adopted for characterizing the winter nighttime latitudinal structure was the standard practice of dividing the 40°–80° CGL range into small latitude boxes for averaging purposes. In our case the box width was ½°, and 30 'mid-night' passes with $Kp \leq 1+$ were used. The results, called average electron density latitudinal profiles, appear in Figure 1. The signature of the trough appears as a broad minimum centered at about 60° CGL. The feature grows progressively weaker with altitude until 950 km, where it is barely discernible. It is possible to recognize clear trends in the variations of the slopes of the different segments comprising the latitudinal structure. Beyond the poleward peak the high-latitude part of Figure 1 shows a small positive slope which changes in a regular manner to a small negative slope as the altitude increases. The trough bottom itself exhibits a similar but more pronounced behavior. Equatorward of the trough, the trend is again one of larger and larger negative slopes as altitude increases.

At the top of Figure 1 we also present the average behavior of h_{max}, the height at which the peak electron density N_{max} occurs. On the average, h_{max} decreases from approximately 360 km at mid-latitudes to about 300 km at high latitudes, most of the decrease occurring at the latitudes occupied by the trough minimum in N_{max}. It should be noted that the derived values of h_{max} are generally considered to be less reliable than the N_{max} values obtained from f_0F_2 scalings.

It is difficult to identify the poleward wall of the trough in Figure 1, in spite of the fact that the poleward wall is the most prominent feature of the trough appearing on most of the individual Isis latitudinal profiles. This points out how simple averaging techniques can smear out significant structure, even when a strictly defined set of criteria is used to define the data to be averaged. Thus the results in Figure 1 could easily be interpreted as indicating that the trough is either weak or nonexistent during magnetically quiet conditions, a conclusion contrary to the majority of the 30 passes used to get Figure 1.

Since the base or foot of the trough's poleward wall is the most consistent and easily recognizable point on the majority

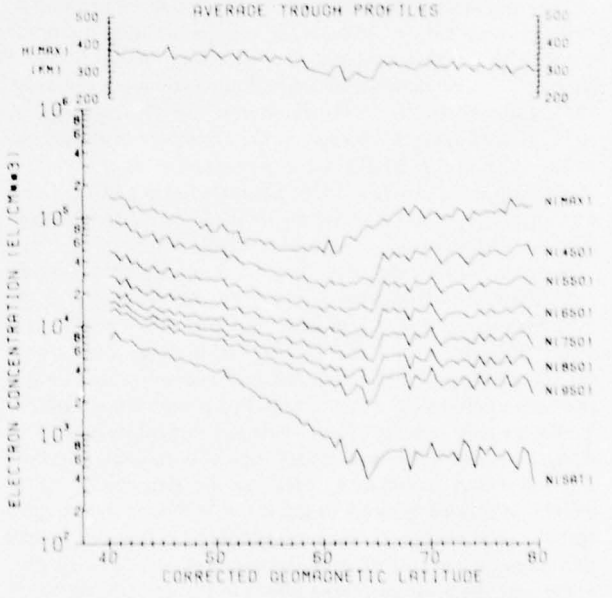

Fig. 2. Latitudinal profiles of the average main trough at eight topside heights, obtained from 23 of the 30 passes used to derive Figure 1. The poleward walls of individual troughs were brought to a common position before averaging electron density values (see text for details). The top panel shows average h_{max} behavior.

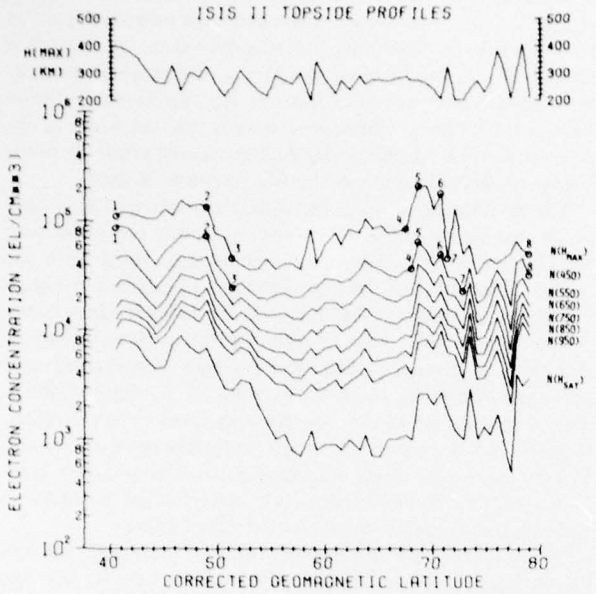

Fig. 3. An individual Isis 2 pass illustrating the parameterization scheme. Data were gathered by the topside sounder between 0608 and 0628 UT on December 18, 1971. The two sets of numbers 1–8 define seven latitude segments of the electron density profile at h_{max} and 450 km. The top panel shows the variation in h_{max}.

of the Isis passes for December 1971 (as was pointed out in the f_0F_2 analysis of *Pike* [1976]), this key position was used in our second averaging attempt. Of the 30 passes used to get Figure 1, seven were not suitable for an unambiguous determination of the poleward wall's position. For the remaining 23 passes the base of the trough wall was selected from the 450-km height data. All of the passes were then shifted in latitude in order to align the trough walls at their mean position of 64.5° CGL, and then the $N_e(h)$ versus latitude profiles were averaged as before. The effect of this procedure is to pick the individual troughs out from the continuum and thus to average the feature of interest rather than the gross latitudinal structure. Figure 2 thus shows more representative average main trough profiles, whereas Figure 1 gives the average electron density latitudinal profile over the 40°–80° CGL range.

An obvious feature of Figure 2 is the well-defined poleward walls of the troughs above 450 km. At h_{max}, however, the trough is not as well defined. We found the reason for this to be that while the base of the poleward wall occurs at generally the same latitude for topside heights, at h_{max} (usually in the 300- to 350-km range) the poleward wall occurs within a few degrees of its 450-km position, and thus averaging a movable feature causes it to be smoothed over.

In order to simplify the overall characterization of the trough we decided to employ a third representation scheme which takes into account both latitude and altitude effects. Each of the Isis 2 passes in the 40°–80° CGL range was divided into seven latitude segments. All of the data points within a given segment were fitted with a straight line, and the slopes and intercepts of the respective straight lines were then averaged. The eight latitudes defining these segments were determined independently at two heights (h_{max} and 450 km). Figure 3 gives an example of this 'parameterization' procedure for the main trough and adjacent features. These are the (1) mid-latitude gradient, (2) equatorward trough gradient, (3) trough minimum, (4) trough poleward wall, (5) auroral peak, (6) auroral peak decline, and (7) polar gradient. Segments 1–5 describe generally well recognized features, while segments 6 and 7 represent an attempt to describe quantitatively the dominant pattern encountered on most of the high-latitude Isis profiles used in our study.

The parameterization of the $N_e(h)$ data above 450 km was carried out by using the eight breakpoints scaled at the 450-km level, a procedure clearly justified by most of the individual passes (for example, see Figure 3) as well as the results presented in Figure 2. The end product of this parameterization scheme appears in Figure 4. In examining these results, note that Figure 4 is essentially a 'linearized' version of Figure 2 for heights above 450 km. There is, in particular, a smooth, regular variation in the slopes of the components of the trough with height.

In Table 1 we list the coordinates of the intersection points of the seven latitude segments at each height in Figure 4. This information may be used to generate readily all of the quantitative features of the baselevel trough depicted in Figure 4.

In order to compare the morphological features in Figure 4 with those determined by other investigators we have indicated the positions of several previously published boundaries of ionospheric, plasmaspheric, and auroral phenomena associated with the 40°–80° CGL range. The specific parameters considered are described in Table 2.

As was stated earlier, the poleward wall of the trough is the most conspicuous feature on virtually all of the Isis passes examined in this study. We found that this feature, identified by points 4 and 5 in Figure 3, does not always change with height in the same systematic way. For example, the ratio of the electron density at point 5 to that at point 4 decreases, remains constant, or increases with height with equal probability. On the average this ratio has a value of 2.15 from 450 km to 950 km. On the other hand, the ratio of the average electron density within the auroral peak to that in the trough minimum diminishes smoothly with altitude as shown in Figure 5. This pattern is basically independent of whether the ratios are determined by using individual passes or the average results presented in Figures 1, 2, and 4.

A related aspect of the height dependence of the latitudinal electron density profiles is the ratio $N(h)/N_{max}$. The average behavior of this quantity from 450 to 1400 km over the 40°–80° CGL range is given in Figure 6.

Note that at all heights up to 950 km the ratios remain basically constant over the 40°–57° CGL range. At 1400 km the transition is smoother and starts at a lower latitude. These results indicate that the shape of the F region $N_e(h)$ profile is invariant from mid-latitudes to approximately the base of the equatorward trough wall. The sharp transition to decreasing $N_e(h)/N_{max}$ values occurs entirely within the trough minimum. Beyond the poleward wall the ratios are again constant, indicating that the average profiles at these high latitudes have the same shape.

DISCUSSION

General trough morphology. Figures 2 and 4 summarize our characterization of the winter nighttime trough for magnetically quiet times. Our parameterization results (Figure 4 and Table 1) describe this baselevel trough in a quantitative way, capable of being compared with results obtained by other workers. The specific points of comparison listed in Table 2 and indicated in Figure 4 need some elaboration. The statistical results of *Feinblum and Horan* [1973] and *Halcrow* [1976] can

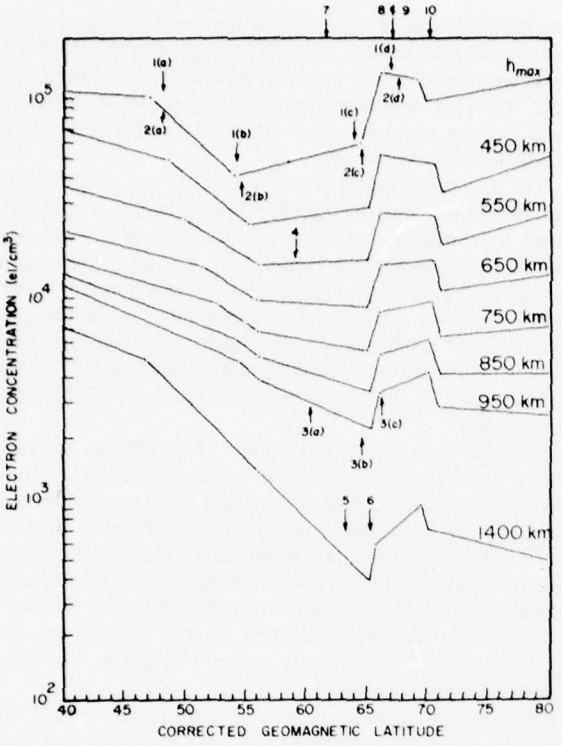

Fig. 4. A representation for the baselevel main trough constructed from 22 of the 30 passes used to derive Figure 1 (for details see text). Table 1 lists coordinates of the intersection points of the seven latitude segments at each of the eight topside heights shown. Comparisons with previous work indicated by numbers 1–10 are listed in Table 2.

be used to generate the four latitude breakpoints defining the trough's equatorward edge, minimum, and poleward walls in peak density. These results, plotted as points 1*a*, 1*b*, 1*c*, and 1*d* and 2*a*, 2*b*, 2*c*, and 2*d* along the $N(h_{max})$ curve, are in remarkably good agreement with the low Kp results presented in Figure 4. The only difference to note is that the width of the poleward wall is smaller in our analysis, owing primarily to the higher spatial resolution of the Isis 2 topside sounder.

The electron densities in the trough minimum at h_{max} have as an average value 5×10^4 el/cm³, a number consistent with the 2-MHz critical frequency usually associated with the trough. The height of the peak density, as described in Figure 1, shows a tendency to decrease over the latitude range dominated by the trough. This is contrary to the usual picture of the trough as a region of low density, high temperature, and consequently high h_{max} (see, for example, *G. N. Taylor* [1973]). The unique aspect of very low Kp associated with our results suggests that the baselevel trough characterized here may not, in fact, have very much enhanced plasma temperature associated with it. We will discuss this point further in regard to possible plasmapause signatures described below.

In comparing the altitude dependence of trough features above h_{max} with that determined by others we note that the *Rycroft and Thomas* [1970] values for the latitude of the trough center and poleward wall boundaries at 1000 km are again in excellent agreement with those presented in Figure 4 (see points 3*a*, 3*b*, and 3*c*). Both the trough's center at 550 km derived from *Tulunay and Sayers'* [1971] analysis (see point 4) and the trough's minimum N_e value of 2.6×10^4 el/cm³ at 400 km [*Chan and Colin*, 1969] are also in good agreement with Figure 4.

Turning to more general altitude-dependent features, we note that the N_e versus latitude gradients from mid-latitudes

TABLE 1. Coordinates of $N_e(h)$ Versus Latitude Segments From Parameterization Analysis

Height, km	Segment Definition Points							
	1	2	3	4	5	6	7	8
h_{max}								
N	10.89	10.12	4.06	5.84	13.37	12.55	9.71	12.76
θ	40.0	46.9	54.1	64.4	66.0	69.1	69.6	80.0
450								
N	6.99	4.88	2.32	2.84	5.23	4.73	3.37	5.15
θ	40.0	48.5	56.1	64.9	66.0	70.4	71.1	80.0
550								
N	3.63	2.49	1.49	1.58	2.70	2.61	1.84	2.62
θ	40.0	49.8	56.1	65.0	66.0	70.4	71.1	80.0
650								
N	2.16	1.44	1.00	0.91	1.49	1.55	1.07	1.30
θ	40.0	51.2	55.8	65.1	66.0	70.3	71.1	80.0
750								
N	1.58	0.94	0.69	0.54	0.86	0.96	0.65	0.72
θ	40.0	52.5	55.8	65.2	65.9	70.3	71.0	80.0
850								
N	1.32	0.64	0.51	0.34	0.53	0.63	0.42	0.42
θ	40.0	54.0	56.0	65.2	65.9	70.1	70.9	80.0
950								
N	1.15	0.49	0.38	0.22	0.34	0.43	0.29	0.26
θ	40.0	54.4	56.1	65.2	65.9	70.0	70.7	80.0
1400								
N	0.72	0.48	0.13	0.04	0.06	0.09	0.07	0.05
θ	40.0	46.8	56.1	65.3	65.7	69.5	70.1	80.0

N is the electron concentration in units of 10^4 el/cm³; θ is the corrected geomagnetic latitude in degrees.

Segment 1–2 is the mid-latitude gradient; segment 2–3 is the equatorward trough gradient; segment 3–4 is the trough minimum; segment 4–5 is the trough poleward wall; segment 5–6 is the auroral peak; segment 6–7 is the auroral peak decline; segment 7–8 is the polar gradient.

TABLE 2. Comparison of Previous Investigations With the Parameterized Baselevel Trough

No.	Reference	Height	LT	$\overline{Kp}$	Feature	Λ, deg
			Ionospheric and Plasmaspheric Comparisons			
1	*Halcrow* [1976]	h_{max}	0000	0.5	(a) top of equatorward trough wall	48.6
					(b) foot of equatorward trough wall	54.2
					(c) foot of poleward trough wall	63.8
					(d) top of poleward trough wall	66.8
2	*Feinblum and Horan* [1973]	h_{max}	0000	0.5	(a) top of equatorward trough wall	48.0
					(b) foot of equatorward trough wall	54.5
					(c) foot of poleward trough wall	64.5
					(d) top of poleward trough wall	67.5
3	*Rycroft and Thomas* [1970]	1000 km	0000	0.5	(a) center of trough	60.3
					(b) foot of poleward trough wall	64.5
					(c) top of poleward trough wall	66.1
4	*Tulunay and Sayers* [1971]	550 km	0200–0300	<3+	center of trough	59.0
5	*Chappell et al.* [1970]	1400 km*	0200	0.5	H^+ plasmapause position	63.2
6	*H. A. Taylor et al.* [1969]	1400 km†	near 0000	0.5	H^+ plasmapause position	65.3
			Comparisons With Related Phenomena			
7	*Aarons and Allen* [1971]	350 km	0000	0.5	average location of F region irregularity boundary determined by scintillation measurements	≈61.5
8	*Sheehan and Carovillano* [1976]		0000	0.5	equatorward edge of aurora for November–December	≈67
9	*Lui et al.* [1975]		0000	0.5	equatorward edge of the diffuse aurora	≈67
10	*Feldstein* [1966]		0000	0.5	midpoint of the 0000 LT segment of the auroral oval	≈70

*L = 6 measured near the equatorial plane corresponds to Λ = 63.2° at 1400 km.
†L = 7 measured near the equatorial plane corresponds to Λ = 65.3° at 1400 km.

to the foot of the poleward wall become increasingly indistinguishable for heights above h_{max}. This tendency for the equatorward edge of the trough to disappear with increasing altitude was noted by *Calvert* [1966] and *Chan and Colin* [1969].

Our results for the poleward wall gradients differ dramatically from those of *Chan and Colin* [1969], owing mainly to the 5° limit on latitude resolution in the earlier study. While Chan and Colin placed the trough minimum at 63° and the poleward peak at 78°, Figure 4 shows that the gradient actually occurs over a much smaller spatial extent. Yet our average poleward wall density ratio of 2.15 over a latitude range of 0.5°–1.5° appears to be smaller than that found by the *Wildman et al.* [1976] study where in situ probe data achieved an even higher spatial resolution. Finally, it may be concluded that by virtually any characterization of the trough employing two gradients separated by a well-defined minimum the trough signature gets weaker with increasing altitude.

Trough's relationship to auroral boundaries. The trough's most prominent feature, its poleward wall or cliff, has long been considered to be the result of particle-induced (auroral) ionization [*Thomas and Dufour*, 1965; *Sharp*, 1966; *Rycroft and Thomas*, 1970]. Our results presented in Figure 4 show that the foot of the poleward wall at h_{max} lies approximately 2½° equatorward of the statistical position of the band of diffuse aurora for low Kp (see points 8 and 9, taken from the studies of *Lui et al.* [1975] and *Sheehan and Carovillano* [1976]). Point 10 in Figure 4 marks the center of the classic Feldstein oval for low Kp, a point about 3° further to the north. For heights above h_{max}, Figure 4 shows a tendency for the foot of the poleward wall to lie closer to the latitude of the equatorward edge of the diffuse aurora. However, the top of the poleward wall (point 5 in our parameterization) lies at very nearly the same latitude at all altitudes. Its approximate location at 66° is 1° equatorward of the diffuse aurora, a value consistent with the work of *Bates et al.* [1973], which reported a 1°–2° separation from the visual aurora.

Trough's relationship to the plasmapause. The plasmapause was first defined by *Carpenter* [1966] in terms of its equatorial morphology. Subsequent in situ satellite measurements [e.g., *Chappell et al.*, 1970] showed that the electron density discontinuity at the equatorial plasmapause is generally a factor of 10^1–10^2 in about one half of an earth radius. If this feature were preserved along a geomagnetic field line, a plasmapause at L = 4 or 5 would manifest itself as some sort of discontinuity over approximately 1.5–2.0 degrees of latitude at ionospheric heights. If the magnitude of the electron density drop across the equatorial plasmapause were preserved in absolute value down to F region heights, a change of even 10^3 el/cm³ would be nearly impossible to detect at h_{max} where ambient densities lie in the 10^4–10^5 el/cm³ range. High in the topside (h > 1000 km), where ambient densities are of nearly

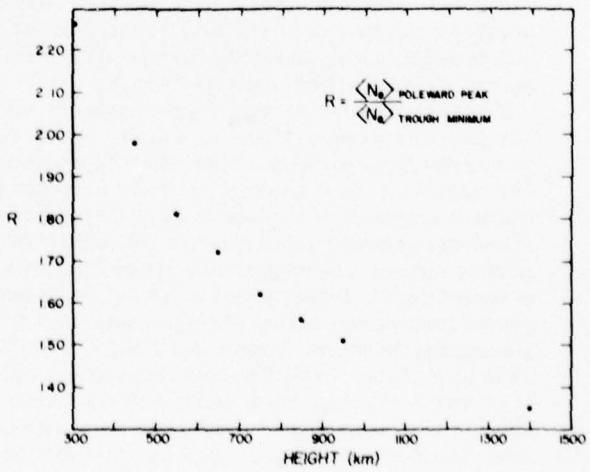

Fig. 5. Altitude dependence of the ratio of the average electron density in the auroral peak to that in the trough minimum determined by using the average results presented in Figure 2.

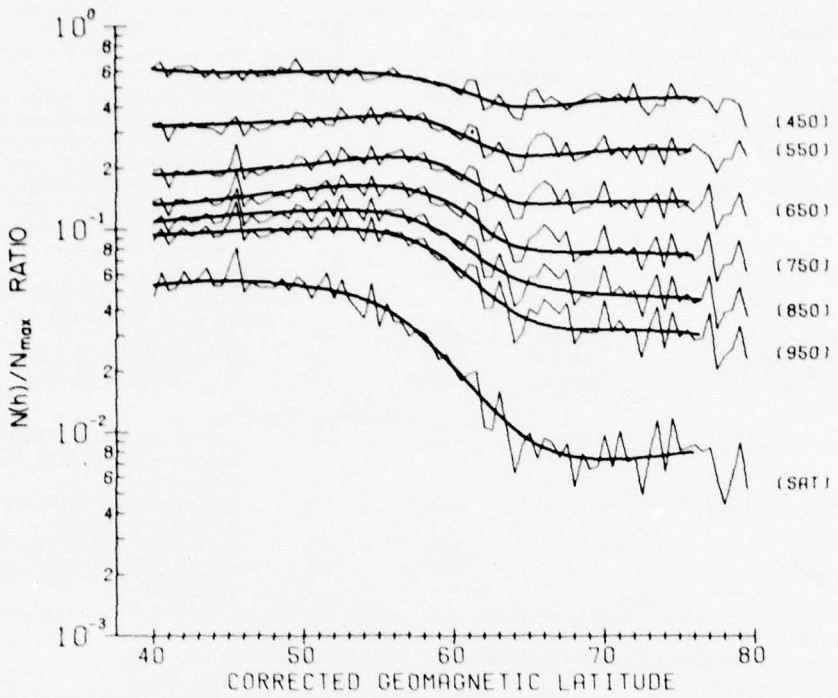

Fig. 6. Average values of the relative electron densities [$N(h)/N_{max}$] for seven topside heights from 450 to 1400 km. The superimposed smooth curves are added for clarity.

the same order as those found in the equatorial plane, a ledge of this magnitude could be detected. Yet perhaps the most striking feature of Figure 4 is that no discontinuity of any appreciable magnitude occurs over the 1½–2 degrees of latitude where the quiet plasmapause would be expected to lie (see points 5 and 6). Only the poleward wall exhibits such a gradient, a feature well understood as resulting from auroral precipitation effects. Thus in spite of the fact that the analysis used to derive Figure 4 accentuated latitudinal gradients there is little or no evidence for an ionospheric manifestation of the plasmapause at the altitudes sampled. It should be emphasized that this conclusion holds for the very quiet geomagnetic conditions under consideration here, since evidence does exist that trough/plasmapause signatures may be found at individual topside heights during disturbed periods (see, for example, the *Norton and Findlay* [1969] Alouette 2 results).

If one examines two or more topside heights at a time, as was done in arriving at Figure 6, then the identification of definite plasmapause effects in the *F* region becomes possible. The $N_e(h)/N_{max}$ ratios displayed in Figure 6 indicate that a relatively sudden change in shape of the topside profiles occurs at latitudes within the trough minimum. Beyond 57° this transition to reduced scale heights seems opposed to most studies of the trough, which find the region to have greatly enhanced plasma temperatures during periods of moderate or active geomagnetic conditions [*Norton and Findlay*, 1969; *Miller*, 1970; *G. N. Taylor*, 1973]. The latitude range over which the quiet time $N_e(h)/N_{max}$ ratios decrease in the present study must therefore mark a rapid transition to increased mean ion mass. Specifically, at latitudes equatorward of 57° the mean ionic mass must be due to a combination of H^+, He^+, and O^+, while beyond 65° the dominant ion must be O^+. This transition zone, occurring most noticeably over the 59°–63° CGL range, marks two ionospheric manifestations of the plasmapause, namely, the light ion trough [*H. A. Taylor*, 1972] and a rapidly increasing 'H^+/O^+ transition height' [*Titheridge*, 1976].

In discussing the h_{max} morphology across the latitudes dominated by the trough we noted earlier that our lower h_{max} values within the trough minimum (see Figure 1) were contrary to the notion that the trough is a low-density high-temperature region. We pointed out above that if any increase in temperature did occur within the trough, its effect upon scale height was overpowered by the influence of mean ionic mass. *G. N. Taylor*'s [1973] incoherent scatter measurements showed the trough to have enhanced plasma temperatures ($T_e + T_i$) by over 1500°K, while *Norton and Findlay*'s [1969] data, obtained during more active conditions, showed T_e increases of nearly 3000°K.

In Figure 7 we present average topside $N_e(h)$ profiles at the four representative latitudes 45°, 52°, 60°, and 67.5°. These may be used to examine the interplay between temperature and ionic mass effects upon the topside scale heights. If one assumes that the $N_e(h)$ slopes at 500 km correspond to purely O^+ scale heights ($H = k(T_e + T_i)/m_i g$), then the derived temperatures show only about a 400°K enhancement from the equatorward edge to the trough minimum (see Table 3). The fact that $N_e(h)/N_{max}$ ratios at 450 and 550 km show a decrease at these latitudes strongly suggests that some light ion depletion occurs at relatively low topside heights. The ($T_e + T_i$) values derived at 45° and 52° are therefore somewhat overestimated. Nevertheless, the temperature differences across the trough would still be quite small in comparison to those reported by *Norton and Findlay* [1969] and *G. N. Taylor* [1973] for more active times. We consider this to reflect the true thermal structure across the latitudes dominated by the trough for the baselevel conditions described here. The temperature we derived for the equatorward edge (≈2760°K) is not incon-

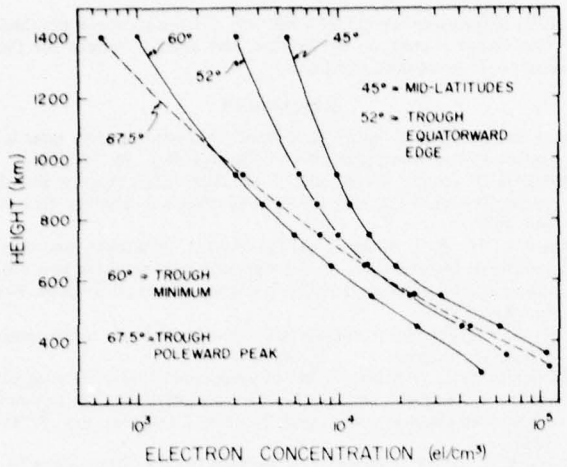

Fig. 7. Average topside vertical electron density profiles for 45°, 52°, 60°, and 67.5° CGL, obtained from the results presented in Figure 2.

sistent with the 3675°K average temperature measured at 500 km at Millstone Hill (≈ 55°) for the nights of December 21–22 and 28–29, 1970 [*Evans and Holt*, 1976], considering that those two periods were a year closer to solar maximum and that magnetic conditions was characterized by $\overline{Kp} = 2$.

In the lower half of Table 3, plasma scale heights at 900 km from the four representative latitudes in Figure 7 show a steady decrease with increasing latitude. Our estimate of the thermal and mean ion mass behavior associated with this pattern assumes (1) the same vertical temperature gradient at 52° as was found by *Evans and Holt* [1976] at Millstone Hill, (2) the latitudinal temperature gradient at 900–1000 km found by *Miller* [1970] and *Titheridge* [1976] for latitudes equatorward of the trough minimum, and (3) a purely O^+ high-latitude domain. The resultant mean ion masses give a H^+/O^+ transition height below 900 km at 45° and slightly above 900 km at 52°. The derived temperatures peak in the trough minimum, the lowest overall value occurring at the latitude of the auroral peak (67.5°).

The H^+/O^+ transition heights of 800–1000 km at mid-latitudes which may be inferred from Table 3 agree with those reported for winter nights by *Titheridge* [1976] and *Davies et al.* [1976]. The rapid increase in transition height found at higher latitudes, which we interpreted as the most obvious *F* region signature of the plasmapause, occurs over the 59°–63° latitude range. This domain falls well within the trough minimum at *F* region heights. The northern terminus of the transition height change, identified as the high-latitude terminus of the relative density decline in Figure 6, correlates well with the statistical position of the plasmapause as given by point 6 [*Chappell et al.*, 1970] in Figure 4. The actual level of the transition height beyond the poleward wall seems to be well above 1000 km in contrast to the value (≈ 900 km) found by *Titheridge* [1976] for slightly more active conditions ($\overline{Kp} = 1.5$).

In summary, the overall pattern for the baselevel trough thus seems to be one of the H^+/O^+ transition height increase beginning a few degrees equatorward of the *L* shell associated with the magnetospheric plasmapause. The change in transition height and the plasma temperature peak both occur within the trough minimum.

A recent study by *Grebowsky et al.* [1976] examined the trough/plasmapause relationship on a case-by-case basis using Isis 2 topside data at 1400 km and Explorer 45 plasmapause detections near the equator for nearly the same winter midnight period described here. Of the 20 cases they examined, two events showed the field line of the equatorial plasmapause definitely at the minimum of the trough, two had the plasmapause poleward of the trough minimum, and 16 cases showed a tendency for the plasmapause field line to lie on the sloping low-latitude side of the N_e trough at 1400 km. These results would, at first, appear to contradict past statistical studies [*Rycroft and Burnell*, 1970; *Rycroft and Thomas*, 1970] which place the plasmapause *L* value in the trough minimum. However, the statistical pattern for the altitude dependence of trough features derived in the present study (see Figure 4) shows that the 'trough minimum' at 1400 km is actually indistinguishable from the 'equatorward edge' of the trough. Thus the *L* value defining the center of the trough minimum in the middle *F* region ($h \approx 500$ km) intersects a much steeper latitudinal gradient at 1400 km. The conclusion of Grebowsky et al., namely, that 'the sloping low latitude side of the trough tended to straddle the plasmapause field line,' is thus in strikingly good agreement with the statistical patterns given in Figures 4, 6, and 7, which show that the plasmapause (defined by the northern terminus of the H^+/O^+ transition height change) falls within the minimum of the *F* region trough [*Brace et al.*, 1974; *Maier et al.*, 1975].

Formation of the trough. The features of the baselevel trough described in previous sections suggest that the trough is

TABLE 3. Representative Scale Height Parameters

Quantity	Mid-Latitudes (45°)	Equatorward Edge (52°)	Trough Minimum (60°)	Auroral Peak (67.5°)
Scale height H at 500 km, km	148	169	193	157
$(T_e + T_i)$,* °K	2414	2757	3149	2561
Scale height H at 900 km, km	661	505	329	247
$(T_e + T_i)$, °K	4000†	4757‡	(4793)	(3598)
$\overline{m_i}$, amu	(6.6)	(10.3)	16§	16§

Values in parentheses are derived quantities.
*Here $m_i = 16$.
†Using *Miller's* [1970] and *Titheridge's* [1976] latitude gradient at 1000 km.
‡Using *Evans and Holt's* [1976] observed $T_e + T_i$ gradient from 500 to 900 km.
§Assumed mean ionic mass (see text).

more pronounced at lower F region heights. *Schunk et al.* [1976] have suggested a mechanism whereby electrodynamic drifts in O^+, possibly of magnetospheric origin, cause enhanced F region loss rates due to velocity-induced increases in the O^+/N_2 ion-atom interchange reaction. Such a process would clearly lead to the trough's being formed more efficiently at heights below the peak of the F region where the N_2 concentrations are high. During the very quiet periods considered in this study, such convection-induced loss effects would migrate toward the poles as long as magnetic quieting persisted. An equatorward edge of the trough extending over a relatively wide latitude range, as found at h_{max} in Figure 4, might well be the consequence of such a process.

For periods of increasing magnetic activity the shrinkage of the plasmapause in the equatorial plane has been described by *Chappell* [1972]. The ionospheric manifestation of this process in the 1400–1800 LT sector would be the appearance of large westward drifts and poleward convection [*Evans*, 1973; *Mendillo*, 1973; *Mendillo and Klobuchar*, 1975]. Both effects would tend to cause the shrinkage of the plasmapause to be simultaneously accompanied by the development of a steeper F region trough at more equatorward latitudes as found by *Tulunay and Sayers* [1971] and *Halcrow* [1976]. As magnetospheric fields penetrate more efficiently to lower altitudes, the trough's equatorward edge and the magnetospheric plasmapause would more nearly lie along the same L shell, in sharp contrast to their lack of correspondence during quiet times. The finding by *Halcrow* [1976] that a well-defined trough exists at midnight only if it has developed prior to 2030 LT lends support to the drift-induced model for trough formation in the dusk sector.

CONCLUSION

The baselevel trough, defined by its occurrence near local midnight (2230–2400) during very quiet magnetospheric conditions ($Kp \leq 1+$) in the middle of winter, is found to have the following characteristics.

1. The trough can be identified frequently (88% of the time) on latitudinal profiles of the topside electron density distribution.
2. The center of the trough is located near 60° CGL, and it has a width of ~10° (2 MHz) at h_{max}.
3. The poleward wall of the trough is steeper than the equatorward wall, their latitudinal extents being ~1½° and ~7°, respectively, at h_{max}. The poleward wall is found 1°–2° lower in latitude than the statistical position of the equatorward edge of the diffuse aurora.
4. The trough gets distorted with increasing altitude, the main effect being a more-or-less monotonic decrease of the electron densities from mid-latitudes to the foot of the poleward wall (~65° CGL).
5. The trough minimum is characterized by moderately high plasma temperatures and decreasing h_{max} values. The latitudes occupied by the trough minimum are marked by a relatively rapid enhancement of the H^+/O^+ transition height.
6. The statistically determined 'plasmapause,' projected to F region altitudes, lies within the trough minimum and coincides with the high-latitude terminus of the transition height change.

Acknowledgments. This work was supported in part by Air Force Geophysics Laboratory (AFGL) contract F19628-75-C-0044 to Boston University. The Canadian Communications Research Centre kindly made available the Isis 2 topside $N_e(h)$ profiles used in this study. We are grateful to Charles Pike of AFGL for his comments and encouragement throughout the course of this work. We also wish to acknowledge Joyce Mendillo for her help with the computer graphics.

The Editor thanks R. W. Schunk and another referee for their assistance in evaluating this paper.

REFERENCES

Aarons, J., and R. S. Allen, Scintillation boundary during quiet and disturbed magnetic conditions, *J. Geophys. Res.*, *76*, 170, 1971.

Bates, H. F., A. E. Belon, and R. D. Hunsucker, Aurora and the poleward edge of the main ionospheric trough, *J. Geophys. Res.*, *78*, 648, 1973.

Brace, L. H., E. J. Maier, J. H. Hoffman, J. Whitteker, and G. G. Shepherd, Deformation of the nightside plasmasphere and ionosphere during the August 1972 geomagnetic storm, *J. Geophys. Res.*, *79*, 5211, 1974.

Calvert, W., Steep horizontal electron density gradients in the topside F layer, *J. Geophys. Res.*, *71*, 3665, 1966.

Carpenter, D. L., Whistler studies of the plasmapause in the magnetosphere, 1, Temporal variations in the position of the knee and some evidence of plasma motions near the knee, *J. Geophys. Res.*, *71*, 693, 1966.

Chan, K. L., and L. Colin, Global electron density distributions from topside soundings, *Proc. IEEE*, *57*, 990, 1969.

Chappell, C. R., Recent satellite measurements of the morphology and dynamics of the plasmasphere, *Rev. Geophys. Space Phys.*, *10*, 951, 1972.

Chappell, C. R., K. K. Harris, and G. W. Sharp, A study of the influence of magnetic activity on the location of the plasmapause as measured by Ogo 5, *J. Geophys. Res.*, *75*, 50, 1970.

Davies, K., R. B. Fritz, and T. B. Gray, Measurements of the columnar electron contents of the ionosphere and plasmasphere, *J. Geophys. Res.*, *81*, 2825, 1976.

Evans, J. V., The causes of storm-time increases of the F-layer at mid-latitudes, *J. Atmos. Terr. Phys.*, *35*, 593, 1973.

Evans, J. V., and J. M. Holt, The combined use of satellite differential Doppler and ground-based measurements for ionospheric studies, *IEEE Trans. Antennas Propagat.*, *AP-21*, 685, 1973.

Evans, J. V., and J. M. Holt, Millstone Hill Thomson scatter results for 1970, *Tech. Rep. 522*, Mass. Inst. of Technol. Lincoln Lab., Cambridge, Mass., May 1976.

Feinblum, D. A., and R. J. Horan, Hilion—A model of the high latitude ionospheric $F2$ layer and statistics of regular ionospheric effects at Ft. Churchill, 1968, report, Bell Lab., Murray Hill, N. J., 1973.

Feldstein, Y. I., Peculiarities in the auroral distribution and magnetic disturbance distribution in high latitudes caused by the asymmetrical form of the magnetosphere, *Planet. Space Sci.*, *14*, 121, 1966.

Grebowsky, J. M., N. C. Maynard, Y. K. Tulunay, and L. J. Lanzerotti, Coincident observations of ionospheric troughs and the equatorial plasmapause, *Planet. Space Sci.*, *24*, 1177, 1976.

Halcrow, B. W., $F2$ peak electron densities in the main trough region of the ionosphere, *Tech. Rep. PSU-IRL-IR-55*, Ionos. Res. Lab., Pa. State Univ., University Park, 1976.

Lanzerotti, L. J., and H. Fukunishi, Relationships of the characteristics of magnetohydrodynamic waves to plasma density gradients in the vicinity of the plasmapause, *J. Geophys. Res.*, *80*, 4627, 1975.

Lanzerotti, L. J., C. G. Maclennan, and H. Fukunishi, Relationships of the characteristics of magnetohydrodynamic waves to plasma density gradients near $L = 4$, *J. Atmos. Terr. Phys.*, *38*, 1093, 1976.

Liszka, L., Variation according to latitude of the electron content of the ionosphere near the auroral zone, *Nature*, *208*, 280, 1965.

Lui, A. T. Y., C. D. Anger, and S.-I. Akasofu, The equatorward boundary of the diffuse aurora and auroral substorms as seen by the Isis 2 auroral scanning photometer, *J. Geophys. Res.*, *180*, 3603, 1975.

Maier, E. J., S. Chandra, L. Brace, J. H. Hoffman, G. G. Shepherd, and J. H. Whitteker, The SAR arc event observed during the December 1971 magnetic storm, *J. Geophys. Res.*, *80*, 4591, 1975.

Mendillo, M., Magnetospheric convection at ionospheric heights, *Tech. Rep. 73-0358*, Air Force Cambridge Res. Lab., Bedford, Mass., June 1973.

Mendillo, M., and J. A. Klobuchar, Investigations of the ionospheric F region using multistation total electron content observations, *J. Geophys. Res.*, *80*, 643, 1975.

Miller, N. J., The main electron trough during the rising solar cycle, *J. Geophys. Res.*, *75*, 7175, 1970.

Muldrew, D. B., F layer ionization troughs deduced from Alouette data, *J. Geophys. Res.*, *70*, 2635, 1965.

Norton, R. B., and J. A. Findlay, Electron density and temperatures in

the vicinity of the 29 September 1967 middle latitude red arc, *Planet. Space Sci., 17*, 1867, 1969.

Pike, C. P., An analytical model of the main *F*-layer trough, Air Force Surveys in Geophysics, no. 348, *Rep. AFGL-TR-76-0098*, Air Force Geophys. Lab., Hanscom Air Force Base, Mass., 1976.

Rycroft, M. J., and S. Burnell, Statistical analysis of movements of the ionospheric trough and the plasmapause, *J. Geophys. Res., 75*, 5600, 1970.

Rycroft, M. J., and S. J. Burnell, Statistical analysis of movements of the ionospheric trough and the plasmapause, *J. Geophys. Res., 75*, 5600, 1970.

Schunk, R. W., P. M. Banks, and W. J. Raitt, Effects of electric fields and other processes upon the nighttime high-latitude *F* layer, *J. Geophys. Res., 81*, 3271, 1976.

Sharp, G. W., Mid-latitude trough in the night ionosphere, *J. Geophys. Res., 71*, 1345, 1966.

Sheehan, R. E., and R. L. Carovillano, The equatorward boundary of the aurora determined from DMSP images (abstract), *Eos Trans. AGU, 57*, 312, 1976.

Taylor, G. N., Structure of the poleward edge of a mid-latitude *F*-region trough, *J. Atmos. Terr. Phys., 35*, 647, 1973.

Taylor, H. A., The light ion trough, *Planet. Space Sci., 20*, 1593, 1972.

Taylor, H. A., Jr., H. C. Brinton, and M. W. Pharo III, Evidence of contraction of the earth's thermal plasmasphere subsequent to the solar flare events of 7 and 9 July, 1966, *Ann. IQSY, 3*, 1969.

Thomas, J. O., and S. W. Dufour, Electron density in the whistler medium, *Nature London, 206*, 567, 1965.

Titheridge, J. E., Plasmapause effects in the topside ionosphere, *J. Geophys. Res., 81*, 3227, 1976.

Tulunay, Y., and J. Sayers, Characteristics of the mid-latitude trough as determined by the electron density experiment on Ariel 3, *J. Atmos. Terr. Phys., 33*, 1737, 1971.

Wildman, P. J. L., R. C. Sagalyn, and M. Ahmed, Structure and morphology of the main plasma trough in the topside ionosphere, paper presented at COSPAR Symposium on Geophysical Use of Satellite Beacon Observations, Boston Univ., Boston, Mass., June 1–4, 1975.

(Received January 31, 1977;
accepted July 12, 1977.)

CHAPTER 3

ELECTRON DENSITY ENHANCEMENTS IN THE F REGION BENEATH THE MAGNETOSPHERIC CUSP

VOL. 82, NO. 29 JOURNAL OF GEOPHYSICAL RESEARCH OCTOBER 1, 1977

Electron Density Enhancements in the *F* Region Beneath the Magnetospheric Cusp

C. C. CHACKO AND MICHAEL MENDILLO

Department of Astronomy, Boston University, Boston, Massachusetts 02215

Electron density enhancements in the topside ionosphere beneath the magnetospheric cusp are consistently observed under an optimum set of geophysical conditions. Average results deduced from Isis 2 topside sounder data show that the cusp-related electron density enhancements maximize at ~77.5° corrected geomagnetic latitude in midwinter near local noon during very quiet magnetospheric conditions. The magnitudes of the enhancements determined at nine topside heights range from a factor of ~2 at h_{max} to ~16 at 1400 km. Enhancements as large as these require *in situ* production at the peak and above, coupled to upward expansion due to the higher plasma temperatures found beneath the cusp. The observed large enhancements further indicate that the ionospheric plasma resides beneath the cusp precipitation long enough (at least a few tens of minutes) for substantial quantities of additional ionization to accumulate. During disturbed periods and in seasons other than midwinter the cusp signature in topside electron densities is, in general, much less well defined or altogether absent.

INTRODUCTION

The entry of magnetosheath plasma into the high-latitude inner magnetosphere through the dayside polar cusps has received considerable attention from a magnetospheric perspective [*Heikkila and Winningham*, 1971; *Frank*, 1971; *Reiff et al.*, 1977]. Related studies have been carried out by workers concerned with the precipitation of soft (<1 keV) magnetosheath electrons and protons into the dayside ionosphere and consequent auroral activity [*Heikkila et al.*, 1972; *Shepherd et al.*, 1976*a*]. We present in this paper characteristics of ionospheric electron density enhancements, perhaps the most direct effect of particle precipitation into the atmosphere, observed in the *F* region directly beneath the magnetospheric cusps [*Oguti and Marubashi*, 1966; *Titheridge*, 1976; *Whitteker*, 1976].

Some of the recent studies of cusp effects upon the ionosphere [*Shepherd et al.*, 1976*b*; *Whitteker*, 1976] used simultaneous satellite measurements (particle fluxes and energy spectra, electron densities, electron and ion temperatures, ion compositions, etc.) to make detailed comparisons of the cause-effect relationships between cusp precipitation and *F* region phenomena. While these investigations have provided a general overview of cusp-related ionospheric effects, the question of whether cusp precipitation leaves a well-defined electron density signature at h_{max} has not yet been fully resolved. The aim of this paper is to investigate this question in detail, using what we feel to be an optimum set of *F* region ionosonde measurements for such a study. In doing this we discuss how various ways of averaging satellite data can modify the quantitative description of a narrow and latitudinally varying feature. We also examine the altitude dependence of topside electron densities beneath the cusp, as well as estimates of topside plasma temperature.

DATA BASE

The ionospheric results reported here were derived from Isis 2 topside sounder data obtained at northern latitudes during December 1971. These data are well suited for studying the purely cusp related electron density enhancements (called CREDE hereafter for convenience) because they represent a remarkably consistent set of observations in terms of the geophysical conditions sampled. All of the December 1971 passes used in this study occurred within 12 days of the solstice, so that the results represent those for which solar production effects at high latitudes would be at their annual minimum. Throughout the period the Isis 2 satellite maintained a nearly noon-midnight orbit (≈1230 h at 60° corrected geomagnetic latitude (CGL), ≈1400 h at 75° CGL), and thus uncertainties about the azimuthal extent of the cusps [*Winningham*, 1972; *Titheridge*, 1976] need not enter into our consideration. The topside soundings were made at a near-constant height of 1400 km over the entire latitude range of interest to us. A relatively rapid data acquisition rate (there are, on the average, about 3 points per 2° latitude interval) enabled us to identify and characterize latitudinal gradients that might otherwise remain undetected or poorly resolved. Nearly half the useful passes available during the 12-day period occurred when the planetary magnetic activity index *Kp* indicated very quiet conditions (*Kp* ≤ 1o). The availability of this narrowly defined data base has enabled us to dispense with the customary need for averaging over large ranges of variables (i.e., solar flux, local time, season, and magnetic activity). The averages reported here should therefore be quantitatively more representative of noontime midwinter cusp-induced *F* region effects during a quiet period.

MAGNETICALLY QUIET PERIODS

Figures 1*a*–1*f* show six Isis 2 passes recorded between December 9 and December 21, 1971. Electron densities obtained from ionograms generated by the topside sounder on board the satellite are plotted as a function of CGL for the eight topside heights h_{max}, 450, 550, 650, 750, 850, 950, and h_{sat} (≈1400) km. The upper panel shows the variation in h_{max} itself. Electron density values less than 10^2 el/cm^3 are not plotted. It should also be pointed out that the derived values of h_{max} are generally considered to be less reliable than the N_{max} values obtained from estimates of f_oF_2. The universal time and local time listed for each pass correspond to those at 60° CGL, and the *Kp* value is the one which prevailed during the 3-hour period that includes the UT quoted above. It should be noted that these six passes with *Kp* values 0o, 0o, 1−, 1−, 1o, and 1o constitute the entirety of midwinter noon-midnight Isis 2 passes offering adequate coverage at northern dayside high

Copyright © 1977 by the American Geophysical Union.

Paper number 7A0587.

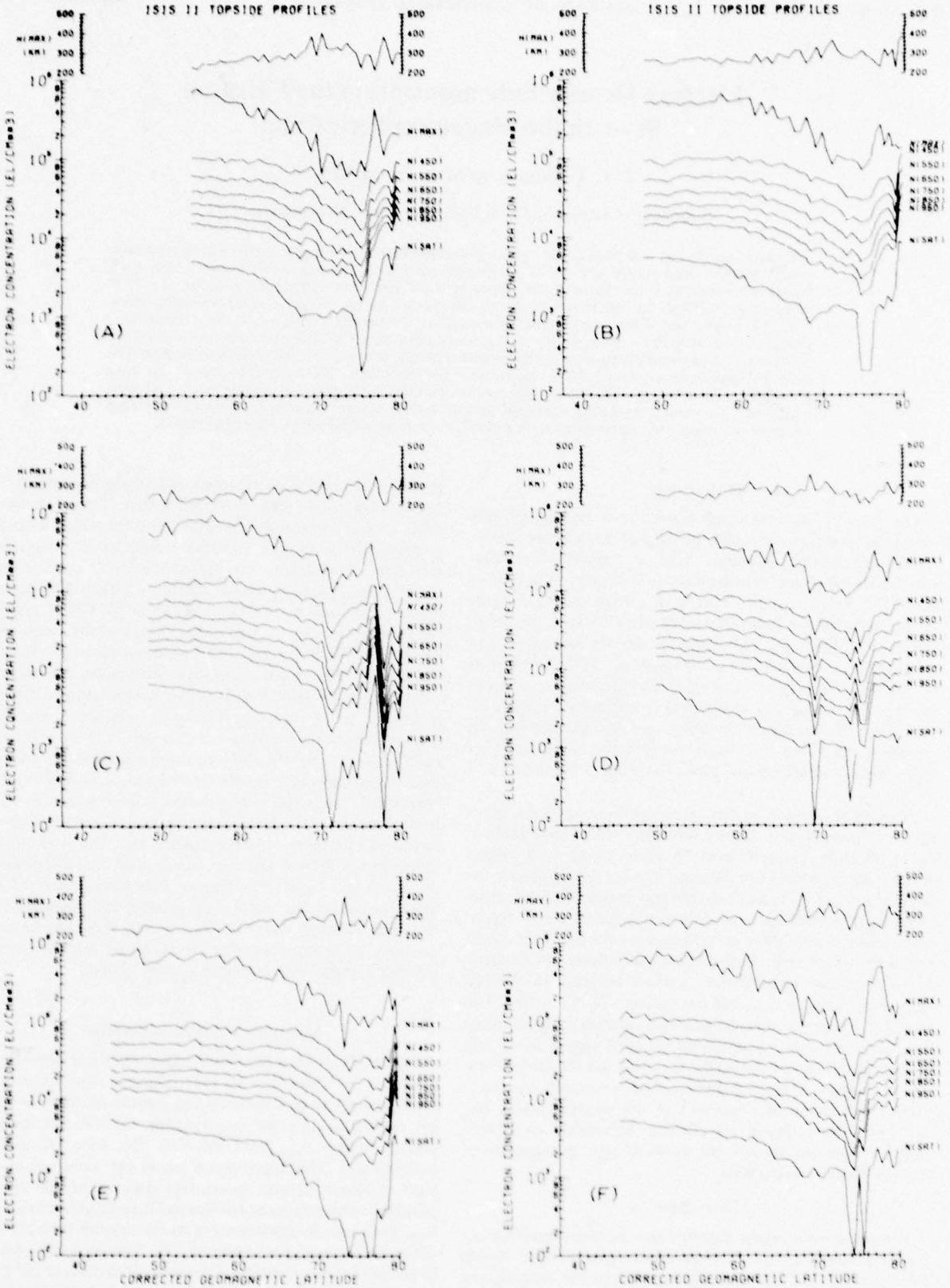

Fig. 1. Six Isis 2 passes in December 1971. Electron density values at eight topside heights are plotted against corrected geomagnetic latitude (CGL). The upper panel shows h_{max}. The UT, MLT, and Kp quoted below for each pass correspond to 60° CGL in the northern hemisphere on the dayside; the solar zenith angle quoted corresponds to the latitude at which the peak in the observed N_{max} enchancement occurs. (*a*) 0707 December 11 (1971), 1232, 0o, 106°; (*b*) 0823 December 10 (1971), 1244, 0o, 106°; (*c*) 0745 December 12 (1971), 1231, 1−, 106°; (*d*) 0745 December 15 (1971), 1220, 1−, 106°; (*e*) 1054 December 11 (1971), 1305, 1o, 103°; (*f*) 0901 December 11 (1971), 1246, 1o, 108°.

latitudes during very quiet ($Ap \leq 1o$) magnetospheric conditions in the December 1971 period.

All six of these passes occurred within the longitude span 18°–78°E, where the corrected geomagnetic latitudes are approximately 5° lower than their corresponding geographic latitudes. Thus at 77° CGL (the expected latitude of the cusp during magnetically quiet periods), calculations for 82° geographic latitude show that sunrise does not occur below a height of 200 km during December solstice conditions. The 'dayside' high-latitude F region beneath the cusp is, in this case, as free of solar production effects as might ever be expected to occur in the northern hemisphere.

An outstanding characteristic of these latitudinal electron density profiles is the remarkable consistency of the features observed. At all heights there is a general tendency for the latitudinal gradient in electron density to be small up to about 60° CGL, where a more severe depletion begins. The electron density reaches a minimum at ≈74° CGL, poleward of which the very steep wall of ionization appears that is to be associated with the magnetosheath particles which precipitate through the cusps. This overall density-versus-latitude pattern has sometimes been called a dayside trough [*Wildman et al.*, 1976] in analogy to the better known 'high/mid-latitude (main) electron density trough' that often appears on the latitudinal profiles of electron density on winter nights.

Figure 1 also shows several aspects of the altitude dependence of the CREDE and associated features. Note, for example, that the onset of the high-latitude enhancement in density occurs at the same latitude at all heights. The minimum which appears just equatorward of the CREDE becomes narrower and deeper at higher heights, an effect which is most pronounced at the satellite height (see Figures 1*a*, 1*b*, 1*e*, 1*f*, and 1*a*, respectively. Note that the coordinates in Figure similar gradients from 450 to 950 km, while at 1400 km a plateau occurs near 70° CGL (see Figures 1*a*, 1*b*, 1*d*, and 1*f*).

Figure 2 (top, middle, and bottom) reproduces spectrograms generated from data gathered by the soft particle spectrometer carried by Isis 2 [*Winningham*, 1972]. These particle measurements were made simultaneously with the topside soundings that led to the electron densities shown in Figures 1*e*, 1*f*, and 1*a*, respectively. Note that the coordinates in Figure 2 are log (electron energy) in electron volts and invariant latitude; Λ differs from CGL by less than ½° (CGL being the larger) at the latitudes of the CREDE depicted in Figure 1. These spectrograms are reproduced here with the limited purpose of pointing out (1) the general coincidence of particle precipitation with the observed electron density enhancements [*Whitteker*, 1976; *Shepherd et al.*, 1976*b*] and (2) the kind of particles responsible for the latter. Representative electron energies seen in the spectrograms are a few hundred electron volts, and the fluxes are a few times 10^9/cm² s sr. The contribution to F region ionization by the soft (<1 keV) proton component in the precipitating plasma is not appreciable [*Shepherd et al.*, 1976*b*].

In addition to the six latitudinally complete satellite passes shown in Figure 1 there were an additional nine passes in

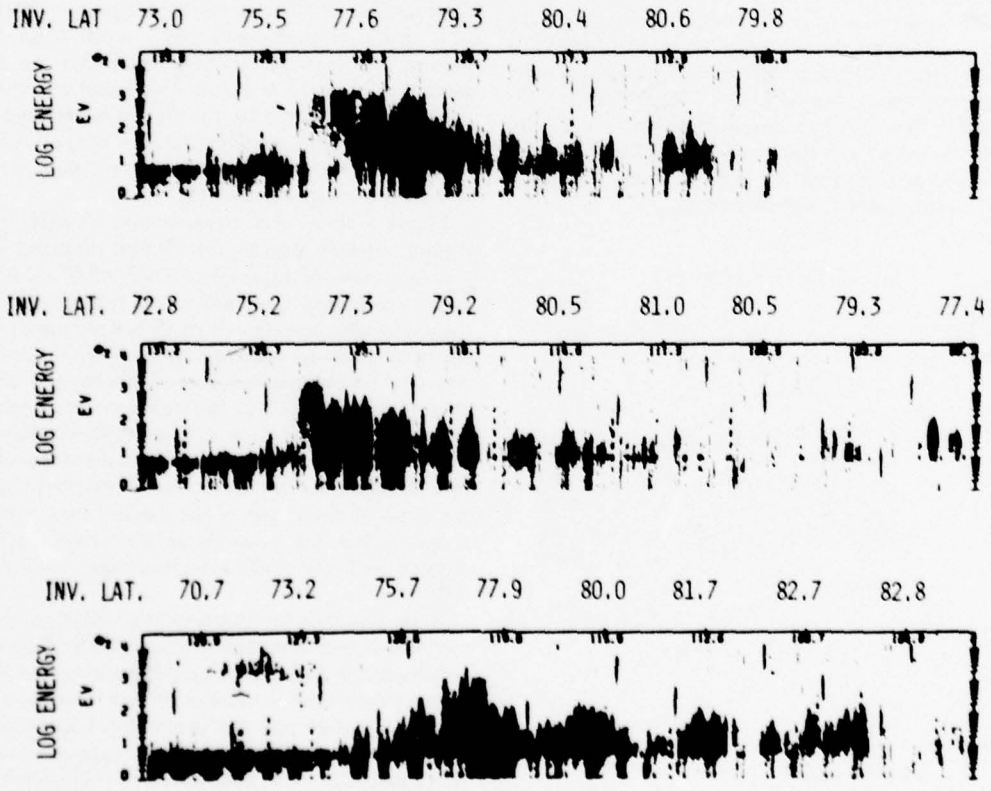

Fig. 2. Electron spectrograms derived from data obtained by the soft particle spectrometer aboard Isis 2. The higher fluxes around 77° invariant latitude indicate precipitating cusp electrons. The particle measurements shown in the top, middle, and bottom spectrograms were obtained 'simultaneously' with the electron density values shown in Figures 1*e*, 1*f*, and 1*a*, respectively.

December 1971 for which Kp was $\leq 1+$ but for which the latitude coverage was incomplete. In each case, however, a clear identification of the onset latitude of cusp-related electron density enhancements could be made. Using this prominent feature, we shifted all 15 passes such that the CREDE onset latitudes were aligned at their average latitude of 75.5° CGL. The data were then averaged by using $\frac{1}{2}$° latitude increments. The results, given in Figure 3, describe the average $N_e(h)$ versus latitude profiles for winter noontime low-Kp conditions across the high-latitude region beneath the cusp.

The average results of Figure 3 preserve all of the characteristic features of the individual passes shown in Figure 1, in particular, the altitude dependence of the electron densities in the various latitude segments. The average behavior of h_{max} across this region is given in the top panel of Figure 3. One can see that a nearly constant value of 245 km extends from midlatitudes to approximately 58° CGL. The relatively sharp decline of N_{max} in the 58°–68° CGL range is accompanied by increasing h_{max} values to approximately 300 km at 68° and beyond.

In spite of the rigidly consistent data base used to obtain Figure 3 there is a certain amount of 'averaging out' of detail seen in the individual passes. Of particular concern is the magnitude of the CREDE as seen in the average versus the individual case. While the 15 passes employed all fell within the Kp = 0o to 1+ range, a truly narrow range by most statistical studies, a simple averaging of this low-Kp set yielded average enhancements that are considerably lower than those presented in Figure 3. The aligned average technique, employed with success for nightside trough morphology [*Pike*, 1976; *Mendillo and Chacko*, 1977], noticeably improved the situation. It should be mentioned, however, that latitude shifts of 0°–2½° had to be used, indicating that even during very quiet intervals the latitudinal position of the CREDE is not constant. Moreover, the latitude range over which the CREDE occurs is also variable, and this too has an effect upon any procedure aimed at specifying the average magnitude of the cusp-related electron density enhancements.

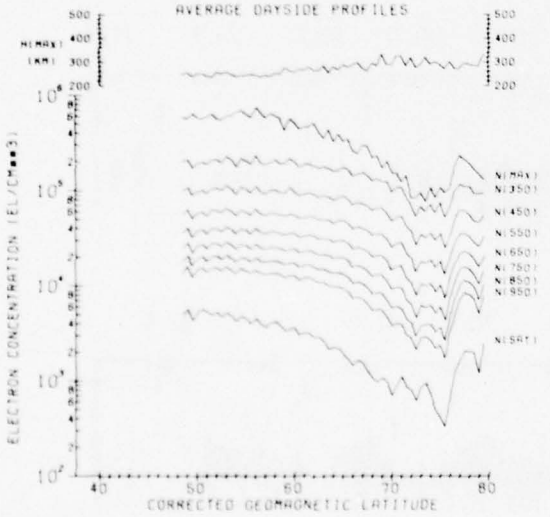

Fig. 3. Latitudinal profiles of the average topside electron density distribution at nine topside heights, obtained by using the six passes shown in Figure 1 plus nine incomplete low-Kp ($\leq 1+$) passes in December 1971. Averaging was done after shifting the minima of all 15 passes to a common mean position.

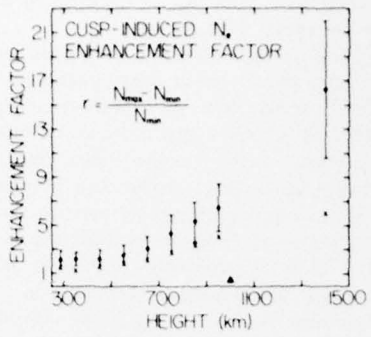

Fig. 4. The enhancement factor $r = (N_{max} - N_{min})/N_{min}$ as a function of altitude. N_{max} is the electron density at the peak of the CREDE, and N_{min} the density at its equatorward minimum. The dot shows the average ratio, and the cross the ratio of the average (see text for details). The triangle represents *Titheridge*'s [1976] result.

The magnitude of the N_e enhancement occurring across the cusp is strongly altitude dependent. We present in Figure 4 the height dependence of an enhancement factor using both 'the feature as seen in the average' and 'the average of the feature.' The quantity plotted is the fractional electron density enhancement $(N_{max} - N_{min})/N_{min}$ at nine topside heights. The upper curve (with the standard deviations indicated) is obtained by determining the ratios for each low-Kp pass and then averaging them. The lower curve shows the ratios calculated by using the already averaged electron density values appearing in Figure 3. The triangle at 1000 km represents the average fractional enhancement of 75% reported by *Titheridge* [1976] on the basis of a statistical study that used a much wider range of the relevant geophysical variables. Note that the three sets of mean results shown in Figure 4 represent a hierarchy of averaging procedures and that the present results give quite significant electron density enhancements at all topside heights in the ionosphere beneath the cusp for the optimum set of geophysical conditions specified earlier.

Figure 5 shows five representative vertical profiles of the topside electron density distribution obtained by using the average results of Figure 3 at 53.5°, 65.0°, 72.0°, 75.5°, and 77.5° CGL. Solar production, considerable at the lowest of these latitudes, diminishes rapidly toward higher latitudes and becomes virtually negligible by 75.5° CGL. Ionization produced by the precipitating magnetosheath particles is found to maximize at 77.5° CGL. We have also made estimates of the plasma temperature $T_e + T_i$ using these average profiles, and Table 1 lists the results. The mean ionic mass of 16 that has been adopted for this computation appears to be justified on the basis of the shape of the profiles themselves as well as recent studies that locate the H^+/O^+ transition height on the dayside well over 1000 km [*Titheridge*, 1976; *Davies et al.*, 1976].

It appears that the characteristic latitudinal profiles of the electron density distribution illustrated in Figures 1*a*–1*f* and represented in Figure 3 invariably occur only in the middle of winter (when solar production at high latitudes is a minimum) under very quiet magnetic conditions. Figures 6*a* and 6*b* and Figures 6*c* and 6*d* show two sets of consecutive passes obtained on October 22, 1971, and March 14, 1973. Perhaps the most striking deviation from Figure 1 that the passes in Figure 6 exhibit is the almost constantly high electron densities that persist even at 75° CGL (and beyond). For example, while all six passes of Figure 1 reach a minimum of $\simeq 10^5$ el/cm^3 at 75°

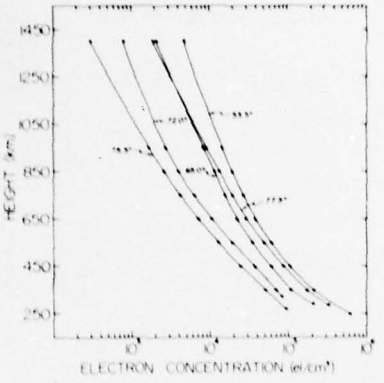

Fig. 5. Average topside vertical electron density profiles for 53.5°, 65.0°, 72.0°, 75.5°, and 77.5° CGL, obtained from the results presented in Figure 3.

CGL at h_{max}, the average N_{max} value at 75° CGL in Figure 6 is $3–4 \times 10^5$ el/cm³, a number more in accord with the N_e values beneath the cusp in Figure 1. Thus it would appear that the state of the background ionosphere may play a critical role in determining whether or not a well-defined CREDE develops. The true seasonal dependence of the CREDE remains to be determined.

Magnetically Disturbed Periods

The dayside high-latitude topside electron density distribution during magnetically disturbed periods exhibits considerably more variations than its quiet time counterpart. A few individual passes serve to illustrate this point.

Figures 7*a*–7*f* give six Isis 2 passes during moderately high Kp ($3o \leq Kp \leq 5o$) periods between December 13 and December 18, 1971. The high degree of consistency apparent in the features of Figures 1*a*–1*f* is not found here. With the exception of Figure 7*a* the signature of cusp precipitation is much less well defined; it is broader and appears at widely varying latitudes. In the case of December 13 (Figure 7*a*) the CREDE is quite narrow (~1°) and very intense. Equatorward of the enhancement, the latitudinal gradient exhibits solar *zenith* angle effects similar to the midwinter period found in Figure 1. Examination of the *z* component of the interplanetary magnetic field showed that B_z changed from a southerly orientation toward the north between 2100 and 2300 UT [*King*, 1975]. Ground-based magnetograms also showed that the satellite pass in Figure 7*a* occurred during the recovery of one of a series of substorms during the day. These changes seem to indicate that the cusp attained its present position after a recent equatorward excursion [*Burch*, 1972; *Yasuhara et al.*, 1973].

Figures 7*b* and 7*c* represent two consecutive passes on December 18 when the IMF maintained a large prolonged northward component and the Kp values were 3o and 5o, respectively. Ill-defined N_e enhancements appear at ~76° CGL on the first pass and at ~78° CGL on the subsequent pass. Note that these latitudes are about the same as the CREDE positions during low-Kp intervals.

Figures 7*d*–7*f* represent three consecutive passes on December 17 when a large magnetic storm was in progress. It is difficult to identify CREDE's on these passes. (IMF data or Isis 2 soft particle spectrograms were not available for this period.) The most outstanding feature on these three successive passes is an unusually sharp negative horizontal gradient at ~67° CGL. It is seen that the feature persists for at least 226 min (the interval between successive Isis passes is ~113 min) without any appreciable latitudinal displacement. The gradient appears at all heights, and its magnitude (Table 2) is one of the highest observed in the December 1971 Isis data set.

Discussion

On the dayside in the middle of winter during magnetically quiet periods the latitudinal profile of the topside electron density distribution behaves in a consistent, well-defined manner. It decreases smoothly from ~60° to ~72° CGL, reaches a narrow minimum centered at ~75° CGL, and rises sharply again, giving rise to a column of ionization centered at ~77.5° CGL. The minimum density appears to reach a 'base level' value of $\sim 10^5$ el/cm³ at h_{max}. Considerations of magnetospheric topology, as well as direct observations of precipitating particles, leave little doubt that the electron density enhancements occur beneath the magnetospheric cusp through which low-energy (<1 keV) magnetosheath plasma finds access to the ionosphere.

The energy spectrum of these precipitating particles is well documented [*Winningham*, 1972; *Doering et al.*, 1976], and therefore cusp precipitation represents a relatively well defined and basically continuous source of charged particles. This provides an opportunity to investigate the physical processes and morphological features associated with the interaction of soft particles and the earth's upper atmosphere. Several studies with this objective have recently appeared [*Shepherd et al.*, 1976*a*, *b*; *Whitteker*, 1976; *Titheridge*, 1976; *Knudsen et al.*, 1977]. Uncertainties about the relative motion of the magnetospheric cusps and the ionospheric plasma are a serious obstacle to establishing a one-to-one correspondence between the cusp precipitation and its various ionospheric effects. Observations and computations show that the horizontal transport of high-latitude ionospheric plasma involves a more or less azimuthal motion and across-the-polar-cap convection [*Jeffries et al.*, 1975; *Heelis et al.*, 1976; *Knudsen*, 1974; *Knudsen et al.*, 1977]. The magnetospheric cusps themselves are known to migrate equatorward in response to changes in the orientation of the interplanetary magnetic field [*Burch*, 1972; *Yasuhara et al.*, 1973]. Furthermore, in the case of the electron density enhancements, one has to allow for at least a few tens of minutes for measurable effects to appear in the topside ionosphere near h_{max} after the cusp precipitation is 'switched on' [*Knudsen et al.*, 1977]. (This implies that the particles 'seen' in the spectro-

TABLE 1. Representative Scale Height Parameters

Quantity	Corrected Geomagnetic Latitude				
	53.5°	65.0°	72.0°	75.5°	77.5°
400-km Height					
Scale height H_i, km	139	143	155	133	170
$T_e + T_i$, °K	2338	2405	2607	2237	2859
700-km Height					
Scale height H_i, km	264	237	191	181	270
$T_e + T_i$, °K	4071	3655	2946	2791	4164
900-km Height					
Scale height H_i, km	358	274	280	235	332
$T_e + T_i$, °K	5221	3996	4084	3427	4915

Here $m_i = 16$.

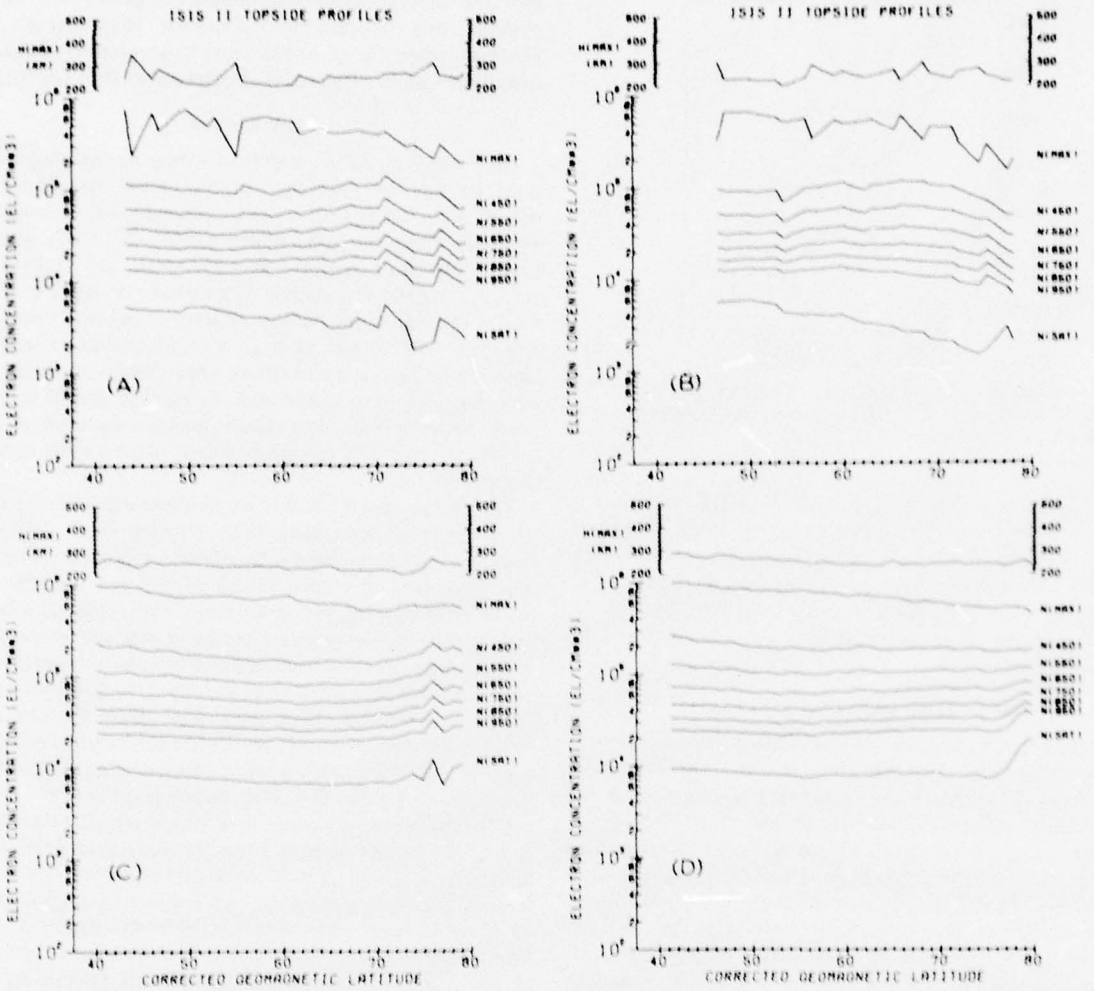

Fig. 6. Same as Figure 1. The solar zenith angle corresponds to the expected latitude of the cusp, calculated by using the relation $\lambda_c(400\text{ km}) = 80 - 2Kp$ deg [*Titheridge*, 1976]. (*a*) 0210 October 22 (1971), 1441, 1 −, 97°; (*b*) 0405 October 22 (1971), 1451, 1o, 09°; (*c*) 1629 March 14 (1973), 1256, 1o, 69°; (*d*) 1823 March 14 (1973), 1208, 0+, 70°.

grams of Figure 2 may not be related in detail to the electron densities shown in the appropriate passes in Figure 1.) Note, however, that if one assumes steady state conditions ($q = \beta N_e$), the production rate of ≈100 el/cm³/s determined by Knudsen et al. for precipitating cusp electrons at the *F* layer peak (≈300 km) and a loss coefficient of 10^{-4}/s [*Rishbeth and Garriott*, 1969] give a density value of 10^6 el/cm³. The observed N_{max} value of $\approx 3 \times 10^6$ el/cm³ indicates that while a static equilibrium may not be achieved, the residence time for plasma beneath the cusp [*Knudsen et al.*, 1977] is sufficiently long to allow appreciable electron density enhancements to occur. It should also be noted in this context that the recently reported small-scale fluctuations in the latitude of the cusp precipitation may account for the considerable amount of latitudinal structure seen in the electron density values equatorward of the CREDE [*Stiles et al.*, 1977].

The average intensity of the CREDE, determined for quiet midwinter conditions (≈200% at h_{max}, rising by more than an order of magnitude at 1400 km), is several times larger than might be expected on the basis of previous statistical results. There is little evidence for significant enhancements near 77° CGL in the average electron density values compiled by *Thomas et al.* [1966] and *Chan and Colin* [1969] using Alouette I data. *Titheridge* [1976], also using Alouette data, found an average enhancement at 1000 km of ≈75%, a value attributable entirely to thermal expansion of the ionosphere. On the other hand, detailed examinations of individual satellite passes [*Hruška et al.*, 1973; *Whitteker*, 1976; *Shepherd et al.*, 1976*b*] have shown enhanced topside electron densities near the cusp location, although there were uncertainties about the occurrence frequency of the enhancements and their dependence on altitude and latitude.

One of the persistent disadvantages with which statistical studies in the past have had to contend is the need for averaging over large ranges of several variables ($F_{10.7}$, LT, season, magnetic activity). For example, in *Titheridge*'s [1976] analysis of quiet time winter conditions, measurements spanning a 3-month period around the December solstices of 1962–1964 were used. The local times sampled were 0900–1600, Kp being in the 0o–3o range. The magnitude of the effect stands a serious risk of being scaled down in the course of such an averaging procedure. It should be borne in mind that the electron density enhancements we have reported pertain to optimum conditions under which the full effect of CREDE, unencumbered by contamination from solar production, is observable. It is also important to point out that the magni-

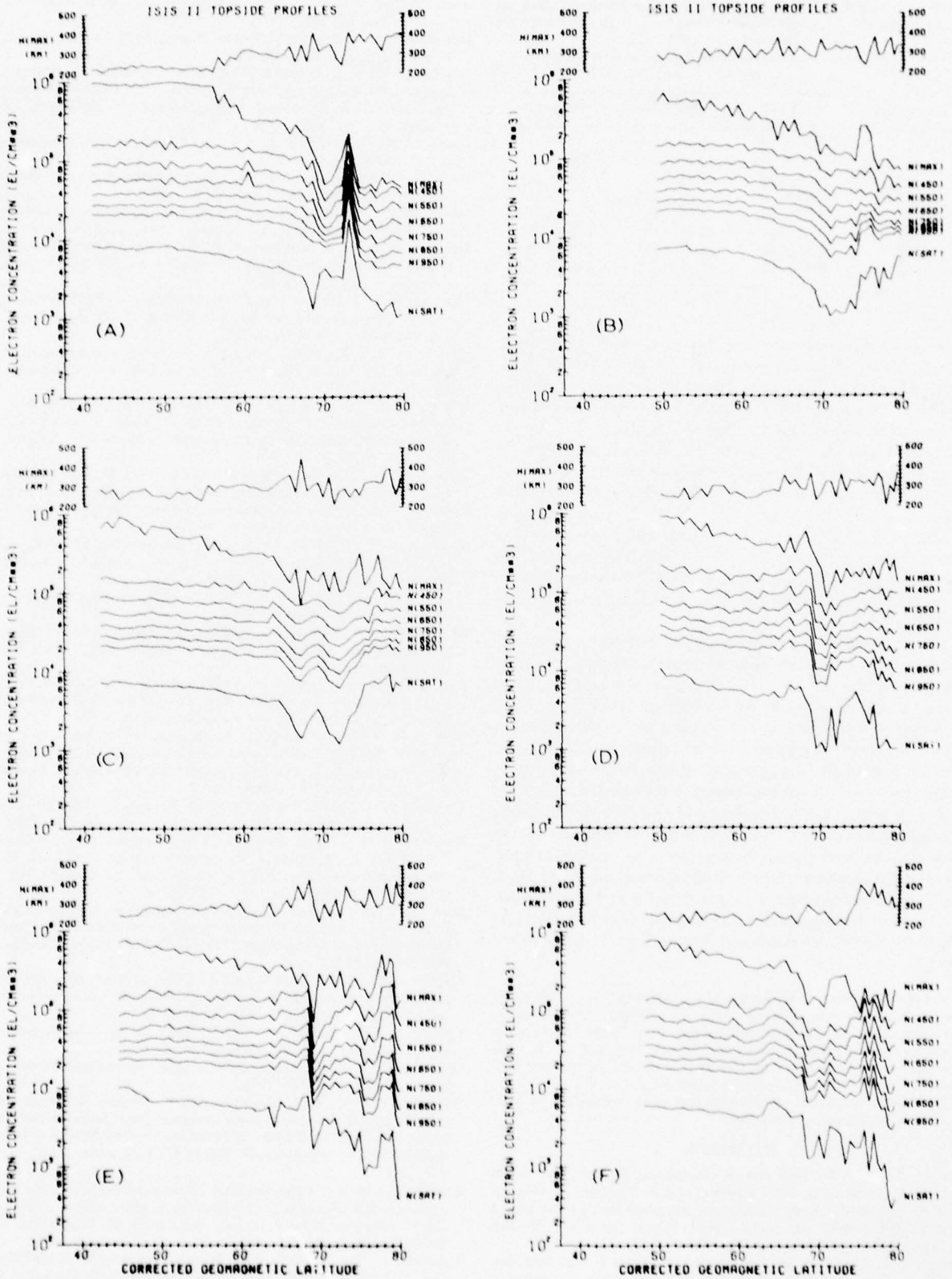

Fig. 7. Same as Figure 1. The solar zenith angle corresponds to the expected latitude of the cusp, calculated by using the relation $\lambda_c(400\ km) = 80 - 2Kp$ deg [*Titheridge*, 1976]. (*a*) 2138 December 13 (1971), 1034, 3+, 97°; (*b*) 0744 December 18 (1971), 1208, 3o, 103°; (*c*) 0938 December 18 (1971), 1226, 5o, 97°; (*d*) 0707 December 17 (1971), 1207, 4+, 100°; (*e*) 0900 December 17 (1971), 1223, 3+, 102°; (*f*) 1053 December 17 (1971), 1241, 3+, 99°.

TABLE 2. Latitudinal Gradients in Topside Electron Densities Observed at 68° CGL on Three Consecutive High-Kp Passes on December 17, 1971

Height, km	$dN_e/d\lambda$, el/cm³ deg CGL		
	0707 UT	0900 UT	1053 UT
h_{max}	1.53×10^5	2.16×10^5	1.58×10^5
450	1.96×10^5	2.41×10^5	5.24×10^4
550	1.05×10^5	1.42×10^5	1.87×10^4
650	6.02×10^4	8.68×10^4	2.10×10^4
750	3.77×10^4	5.60×10^4	1.71×10^4
850	2.57×10^4	3.84×10^4	1.54×10^4
950	1.85×10^4	2.78×10^4	1.37×10^4
1400	3.40×10^3	1.03×10^4	5.40×10^3

tude of the observed enhancements near the F region peak calls for bona fide in situ production. Heat conduction from higher altitudes and consequent upward expansion of the ionosphere [*Titheridge*, 1976] probably contribute to the still larger enhancements found at higher altitudes.

Temperatures ($T_e + T_i$; see Table 1) deduced from the scale heights ($H = k(T_e + T_i)/m_i g$) of the average vertical electron density profiles shown in Figure 6 (Table 1) are lower than those found by *Titheridge* [1976]. Note, however, that the latitudinal and vertical gradients in temperature are quite similar to those reported in the above study. In particular, the temperatures at the cusp latitudes (~77.5° CGL) are substantially higher, at all heights, than those just equatorward of the cusp.

The main reason for the generally ill defined nature of the electron density enhancements observed during disturbed periods may be the relatively rapid equatorward migration of the cusps, i.e., the ionospheric plasma does not reside beneath the cusp long enough (a few tens of minutes) for intense ionization peaks to appear. If convection is enhanced during magnetic activity, this effect is augmented. (Conversely, during prolonged quiet periods the cusp occupies its poleward extremum, and large amounts of ionization build up.) At lower latitudes, two additional sources may lend further complexity to the latitudinal electron density distribution: solar ultraviolet radiation and precipitating hard auroral particles [*Hartz and Brice*, 1967], the latter having been injected on the nightside in association with magnetospheric substorms and drifted azimuthally to the dayside [*DeForest and McIlwain*, 1971; *Berkey et al.*, 1974].

Acknowledgments. This work was supported in part by Air Force Geophysics Laboratory contract F19628-75-C-0044 to Boston University. The Canadian Communications Research Centre kindly made available the Isis 2 topside $N_e(h)$ profiles used in this study. The Isis soft particle spectrograms (courtesy of J. D. Winningham) were provided by the Air Force Geophysics Laboratory.

The Editor thanks W. B. Hanson and J. H. Whitteker for their assistance in evaluating this paper.

REFERENCES

Berkey, F. T., V. M. Driatskiy, K. Henriksen, B. Hultqvist, D. H. Jelly, T. I. Shchuka, A. Theander, and J. Ylinemi, A synoptic investigation of particle precipitation dynamics for 60 substorms in IQSY (1964–1965) and IASY (1969), *Planet. Space Sci.*, *22*, 255, 1974.

Burch, J. L., Precipitation of low-energy electrons at high latitudes: Effects of interplanetary magnetic field and dipole tilt angle, *J. Geophys. Res.*, *77*, 6696, 1972.

Chan, K. L., and L. Colin, Global electron density distributions from topside soundings, *Proc. IEEE*, *57*, 990, 1969.

Davies, K., R. B. Fritz, and T. B. Gray, Measurements of the columnar electron contents of the ionosphere and plasmasphere, *J. Geophys. Res.*, *81*, 2825, 1976.

DeForest, S. E., and C. E. McIlwain, Plasma clouds in the magnetosphere, *J. Geophys. Res.*, *76*, 3587, 1971.

Doering, J. P., T. A. Potemra, W. K. Peterson, and C. O. Bostrom, Characteristic energy spectra of 1- to 500-eV electrons observed in the high-latitude ionosphere from Atmosphere Explorer C, *J. Geophys. Res.*, *81*, 5507, 1976.

Frank, L. A., Plasma in the earth's polar magnetosphere, *J. Geophys. Res.*, *76*, 5202, 1971.

Hartz, T. R., and N. M. Brice, The general pattern of auroral particle precipitation, *Planet. Space Sci.*, *15*, 301, 1967.

Heelis, R. A., W. B. Hanson, and J. L. Burch, Ion convection velocity reversals in the dayside cleft, *J. Geophys. Res.*, *81*, 3803, 1976.

Heikkila, W. J., and J. D. Winningham, Penetration of magnetosheath plasma to low altitudes through the dayside magnetospheric cusps, *J. Geophys. Res.*, *76*, 883, 1971.

Heikkila, W. J., J. D. Winningham, R. H. Eather, and S.-I. Akasofu, Auroral emissions and particle precipitation in the noon sector, *J. Geophys. Res.*, *77*, 4100, 1972.

Hruška, A., I. B. McDiarmid, and J. R. Burrows, Ionospheric structure near the dayside boundary of closed field lines, *J. Geophys. Res.*, *78*, 2311, 1973.

Jeffries, R. A., W. H. Roach, E. W. Hones, E. M. Wescott, H. C. Stenbaek-Nielsen, T. N. Davis, and J. D. Winningham, Two barium plasma injections into the northern magnetospheric cleft, *Geophys. Res. Lett.*, *2*, 285, 1975.

King, J. H., Interplanetary magnetic field data 1963–74, *Rep. UAG-46*, World Data Center A for Solar-Terr. Phys., Boulder, Colo., 1975.

Knudsen, W. C., Magnetospheric convection and the high-latitude F_2 ionosphere, *J. Geophys. Res.*, *79*, 1046, 1974.

Knudsen, W. C., P. M. Banks, J. D. Winningham, and D. M. Klumpar, Numerical model of the convecting F_2 ionosphere at high latitudes, *J. Geophys. Res.*, *82*, in press, 1977.

Mendillo, M., and C. C. Chacko, The base level ionospheric trough, *J. Geophys. Res.*, *82*, in press, 1977.

Oguti, T., and K. Marubashi, Enhanced ionization in the F_2 region around geomagnetic noon in high latitudes, *Rep. Ionos. Space Res. Jap.*, *20*, 96, 1966.

Pike, C. P., An analytical model of the main F-layer trough, Air Force Surveys in Geophysics, no. 348, *Rep. AFGL-TR-76-0098*, Air Force Geophys. Lab., Hanscom Air Force Base, Mass., 1976.

Reiff, P. H., T. W. Hill, and J. L. Burch, Solar wind plasma injection at the dayside magnetospheric cusp, *J. Geophys. Res.*, *82*, 479, 1977.

Rishbeth, H., and O. K. Garriott, Introduction to Ionospheric Physics, p. 171, Academic, New York, 1969.

Shepherd, G. G., F. W. Thirkettle, and C. D. Anger, Topside optical view of the dayside cleft auroras, *Planet. Space Sci.*, *24*, 937, 1976a.

Shepherd, G. G., J. H. Whitteker, J. D. Winningham, J. H. Hoffman, E. J. Maier, L. H. Brace, J. R. Burrows, and L. L. Cogger, The topside magnetospheric cleft ionosphere observed from the Isis 2 spacecraft, *J. Geophys. Res.*, *81*, 6092, 1976b.

Stiles, G. S., E. W. Hones, Jr., J. D. Winningham, R. P. Lepping, and B. S. Delana, Ionosonde observations of the northern magnetospheric cleft during December 1974 and January 1975, *J. Geophys. Res.*, *82*, 67, 1977.

Thomas, J. O., M. J. Rycroft, and L. Colin, Electron densities and scale heights in the topside ionosphere: Alouette I observations in midlatitudes, *NASA Spec. Publ.*, *3026*, 1966.

Titheridge, J. E., Ionospheric heating beneath the magnetospheric cleft, *J. Geophys. Res.*, *81*, 3221, 1976.

Whitteker, J. H., The magnetospheric cleft—Ionospheric effects, *J. Geophys. Res.*, *81*, 1279, 1976.

Wildman, P. J. L., R. C. Sagalyn, and M. Ahmed, Structure and morphology of the main plasma trough in the topside ionosphere, paper presented at Cospar Symposium on Geophysical Use of Satellite Beacon Observations, Boston Univ., Boston, Mass., June 1–4, 1976.

Winningham, J. D., Characteristics of magnetosheath plasma observed at low altitudes in the dayside magnetospheric cusps, in *Earth's Magnetospheric Processes*, edited by B. M. McCormac, D. Reidel, Hingham, Mass., 1972.

Yasuhara, F., S.-I. Akasofu, J. D. Winningham, and W. J. Heikkila, Equatorward shifts of the cleft during magnetospheric substorms as observed by Isis 1, *J. Geophys. Res.*, *78*, 7286, 1973.

(Received February 23, 1977;
accepted June 23, 1977.)

CHAPTER 4

THE EQUATORWARD EDGE OF THE DIFFUSE AURORA AND THE POLEWARD WALL OF THE MAIN ELECTRON DENSITY TROUGH: CASE STUDY INVESTIGATIONS

We found ten ISIS-2 passes in December 1971 for which DMSP images were available in near simultaneity. Values of the indices K_p and AE (hourly maximum) shown in Table 4.1 indicate that passes during periods of relative magnetic quiet predominate the set of available December 1971 case-study events [Mendillo and Chacko, 1977]. The approximate UT at which the satellite crossed the 65^{o}N corrected geomagnetic latitude on the night side is used to identify the pass. Note that the pairs of nominally simultaneous passes range from one with $\Delta T = -8$ minutes (i.e., ISIS-2 crossed 65^{o}N CGL on the night side 8 minutes ahead of the DMSP satellite) to one with $\Delta T = +40$ minutes. For all ten cases, the local time period sampled by both satellites was 2230 -0130 hours.

Table 4.1 shows the poleward wall of the trough always equatorward of the equatorward edge (latitude ϕ_a) of the diffuse aurora as seen on the DMSP images. The mean separation between the foot of the poleward wall and the auroral boundary is 4.7^{o} while that between the peak of the wall and ϕ_a is 2.4^{o}, the standard deviations being 1.2^{o} and 1.1^{o} respectively. In summary, Table 4.1 shows that the separation ($\Delta\phi$) between the trough's poleward wall (ϕ_{pw}) and the equatorward edge of the continuous aurora (ϕ_a) as monitored by the DMSP technique is, on

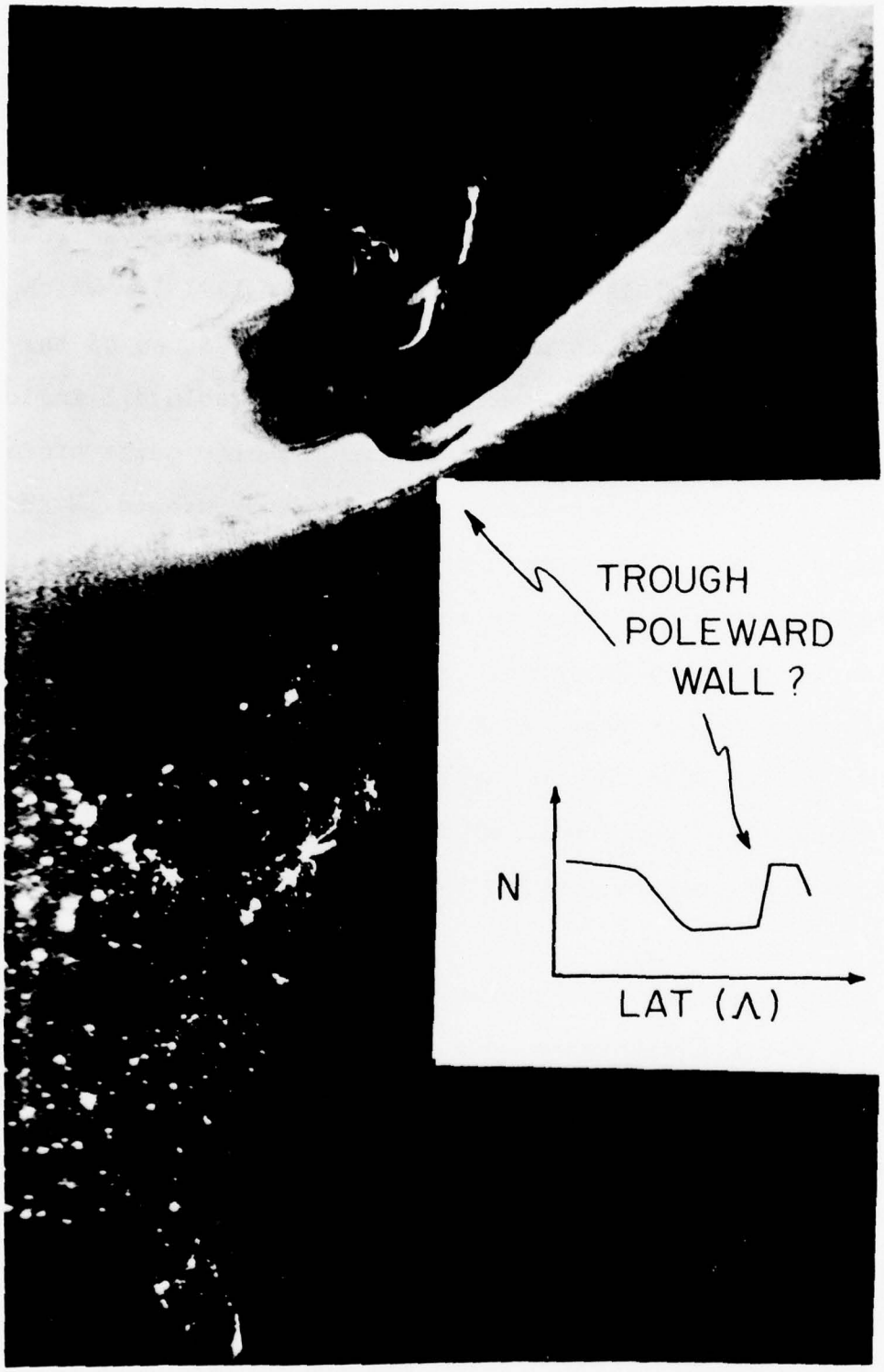

FIGURE 4.1 Sample DMSP auroral image illustrating possible relationship between equatorward edge of diffuse aurora and poleward wall of main ionospheric trough.

TABLE 4.1 Summary of Ten Case-study Investigations Using Simultaneous DMSP/ISIS 2 Data

DATE	UT DMSP	UT ISIS-2	ΔT (min)	K_p	(γ)	LATITUDE OF EQUATORWARD EDGE OF DIFFUSE AURORA (DMSP) ϕ_a (Geog.)	ϕ_a (CGL)	LATITUDE OF POLEWARD WALL OF TROUGH (ISIS-2 ϕ_{pw} FOOT (Geog.)	FOOT (CGL)	TOP (Geog.)	TOP (CGL)	Δφ FOOT	Δφ TOP
Dec 9	0405	0419	+14	3-	87	53.0	65.8	50.2	63.0	51.7	64.5	2.8	1.3
Dec 9	0546	0612	+26	3-→1	119→50	57.5	68.1	51.0	61.8	53.9	64.8	6.3	3.3
Dec 9	0728	0803	+35	1	39→53	63.0	67.2	60.1	64.5	63.0	67.2	2.7	0.0
Dec 10	0903	0840	-23	0	27→37	69.0	70.4	63.0	64.8	66.6	68.2	5.6	2.2
Dec 11	0655	0725	+30	0	32→29	61.0	67.0	55.4	61.6	57.6	63.8	5.4	3.2
Dec 11	0837	0917	+40	0→1	23→38	70.0	69.2	63.8	63.5	67.5	66.2	5.7	3.0
Dec 12	0821	0801	-20	1-	37	63.0	66.4	57.9	61.6	60.1	63.7	4.8	2.7
Dec 12	1002	0954	-08	1-	48→34	69.2	66.8	65.3	63.0	66.8	64.5	3.8	2.3
Dec 19	0806	0838	+32	3+	559	62.0	61.7	56.5	56.3	58.7	58.5	5.4	3.2
Dec 21	0605	0551	-14	1	56	60.0	67.9	55.6	63.6	56.3	65.1	4.3	2.8
			mean				67.05		62.37		64.7	4.68	2.40
			standard deviation				2.32		2.41		2.61	1.24	1.04

the average, 3½ degrees. This separation is somewhat larger than that found in Chapter 2 where long-term auroral statistics were compared with the "Base-Level Trough".

Below we examine several of the "case study" events in detail. The first event offers the most well-defined examples of both DMSP and ISIS 2 observations among the ten near-simultaneous events examined. The third event comprises two sets of successive passes of each satellite. The second case represents a period in which extensive and co-ordinated observations on several related phenomena in the night-time ionosphere have been reported [eg. Whalen et al., 1977; Pike et al., 1977; Weber et al., 1977].

December 21, 1971
DMSP pass at 0605 UT, ISIS 2 pass at 0551 UT,
K_p = 1, AE = 56.

Although the K_p and AE indices indicate near-quiet conditions (and the most recent substorm had a 500γ (AE) intensity and had completely recovered by 2300 UT on December 20, 1971), examination of individual magnetograms revealed recurrent magnetic perturbations between 0520 and 0700 UT at Fort Churchill. The DMSP image (Figure 4.2) shows quiet auroral arcs apparently embedded in the diffuse aurora whose equatorward edge more or less closely follows the 68° CGL curve. The DMSP image covers the magnetic local time range ~ 2300 to 0100 hrs. The ISIS 2 track appears close to the left hand edge of the photograph (see Figure 4.4) where the Van Rhijn effect introduces an element of uncertainty into the determination of the diffuse aurora's equatorward boundary (ϕ_a). However, in the middle region of the image,

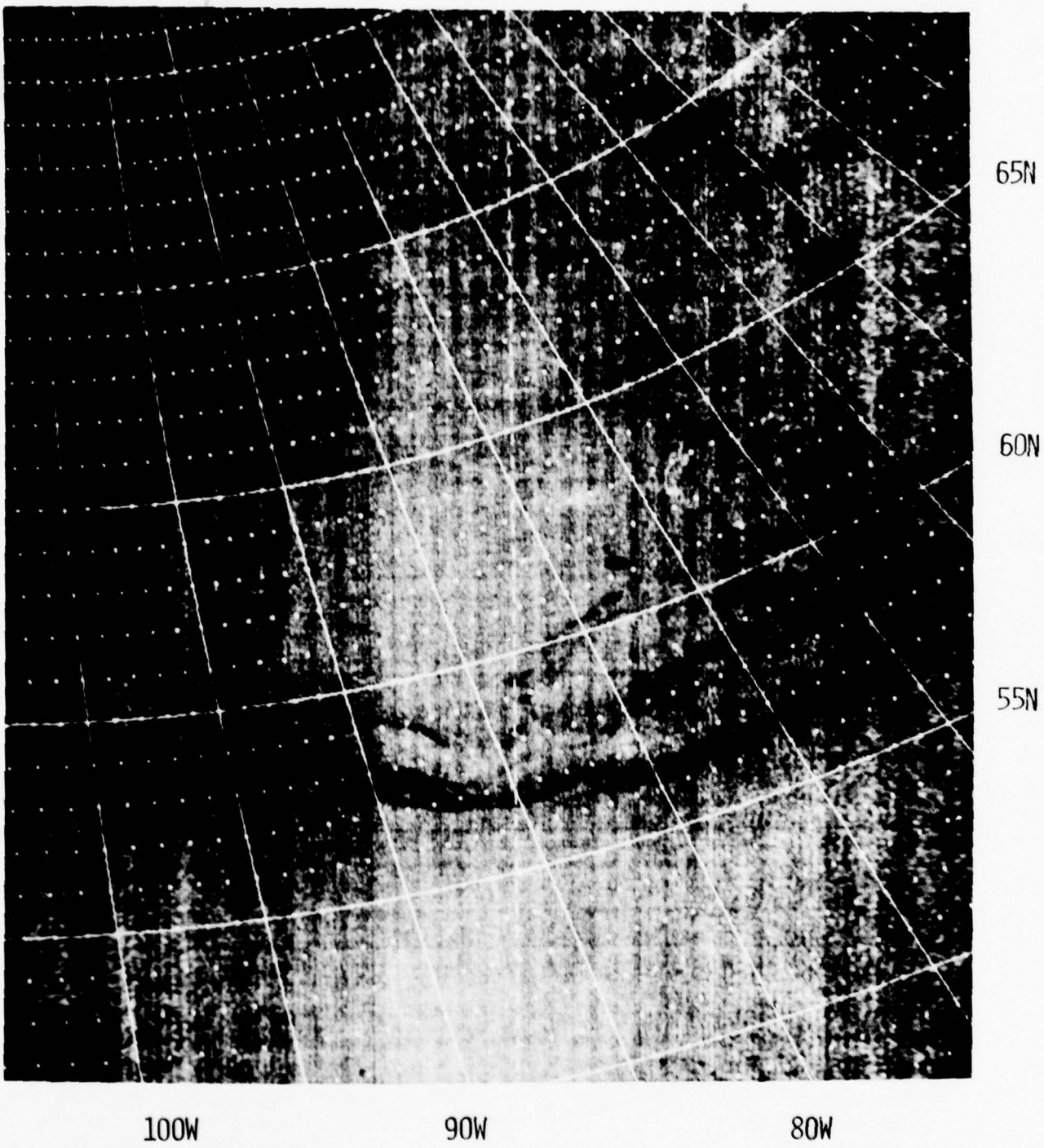

FIGURE 4.2 DMSP image of part of the night side auroral region in the northern hemisphere recorded about 0605 UT on December 21, 1971. Geographic coordinates (100 km) are overlaid.

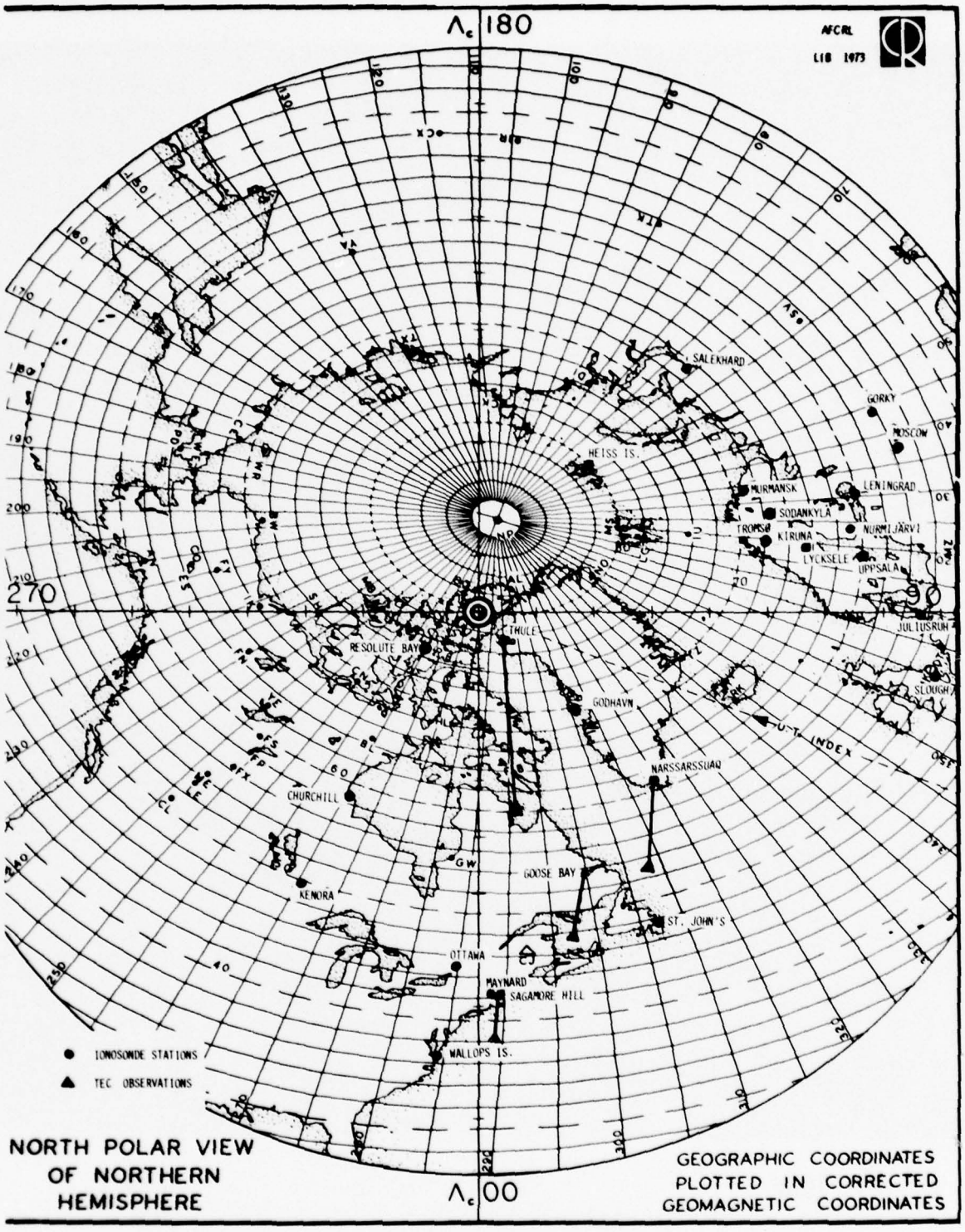

FIGURE 4.3 Polar view of northern hemisphere with geographic coordinates plotted in Corrected Geomagnetic Coordinates. Ionosonde stations(•) and TEC observing sites (▲) used in "case study events" are indicated. Corrected Geomagnetic Latitudes (CGL) appear as concentric circles in subsequent figures.

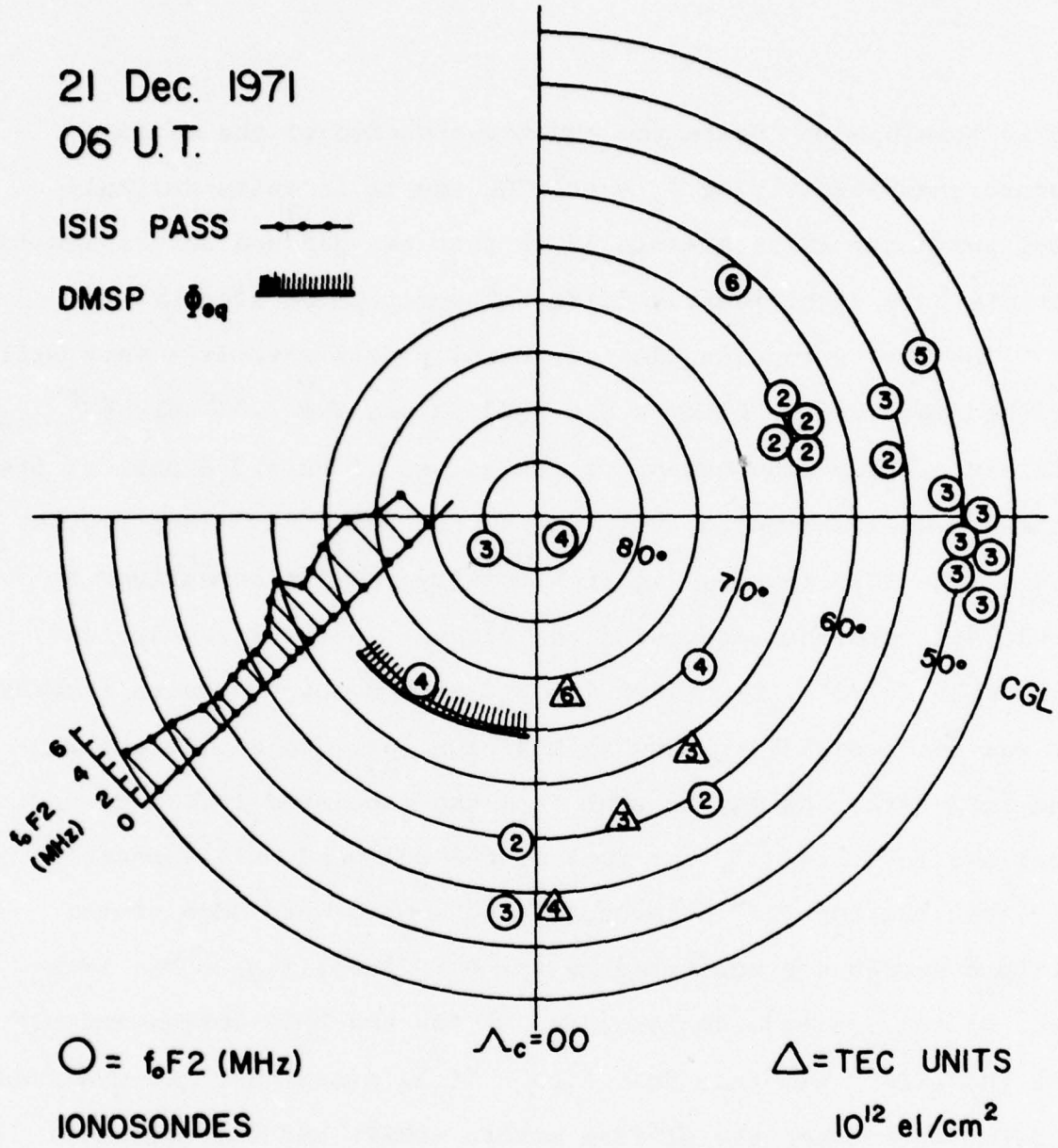

FIGURE 4.4 North polar view in CGL showing the location of near-simultaneous ISIS and DMSP satellite data for 0600 UT on 21 December 1971. Ground-based foF2 values and TEC data at 0600 UT from the network shown in Figure 4.3 are presented using integer values.

it is possible to locate the equatorward edge of the diffuse aurora unambiguously at $\phi_a = 68^o$ CGL and it is quite unlikely [Lui and Anger 1973; Akasofu 1974] that the diffuse aurora should deviate to a significantly different position at 2200 LT.

The ISIS 2 topside electron density data reveals a very well-defined main trough with ~ 2 MHz foF2 values from ~ 53^o to ~ 63^o CGL and a sharp enhancement of ionization (foF2 = 2-3 MHz) at its poleward wall extending from ≈63^o CGL to ≈65^o CGL. (See Figure 4.4). The ISIS topside electron density results summarized in Table 4.1 were obtained using the highest latitude resolution available (≈$2/3^o$). In Figure 4.4 and subsequent composite figures, it was not possible to show such a high latitude resolution in the foF2 data. As may be seen from the tabulated ISIS data scalings in Table 4.1, the foot of the poleward wall appears 4.3^o and the top 3.6^o poleward of the equatorward edge of the diffuse aurora (as monitored by the DMSP satellite). The accuracy of the latitude scalings is ~ $\frac{1}{2}^o$ for the DMSP images and $\leq 1^o$ for the ISIS 2 electron densities. It is clear that the observed separation between the diffuse aurora (DMSP) and the poleward wall of the main electron density trough is physically significant.

Given the observed $\Delta\phi$ at the ISIS sub-satellite location, we were interested in determining the longitudinal (or local time) consistency of the separation over the region covered by the DMSP photograph, and indeed beyond. This is not a simple

question to answer since no F-region monitoring technique can provide ISIS-type latitude resolution at points to the east and west of a given ISIS pass. We turned to the ground-based network of ionosonde sites (via WDC-A) and to the AFGL chain of total electron content (TEC) observing stations (courtesy of J. A. Klobuchar) for supporting data to estimate the spatial consistency of the trough's location away from the ISIS longitude. Figure 4.3 shows the network of 24 ionosondes and the 4 TEC sites used in the study.

In Figure 4.4, a composite view is presented of the DMSP auroral boundary in relation to ISIS topside sounder foF2 values, bottomside foF2 data and satellite beacon observations of TEC for 0600 UT on 21 December 1971. For this case, the ISIS pass occurred several degrees to the west of the DMSP field of view. As shown in Table 4.1, the foot of the trough's poleward wall (at the ISIS pass longitude) is about 4^{o} equatorward of ϕ_a in the DMSP photograph. The only ionosonde station furnishing foF2 data within the DMSP field of view (i.e., Churchill) shows foF2= 4MHz, a value consistent with its location within the poleward wall (as defined by the ISIS data further to the west). For regions to the east of the DMSP data, a trough in foF2 (at≈2MHz) and in TEC (at≈3×10^{12}el/cm^2) appears along the 60^{0}CGL line. Thus, throughout the North American sector, the ionosonde and TEC data support the local time consistency of $\Delta\phi\approx4^{o}$ within (and several hours to the east of) the DMSP field of view. In fact, a trough minimum of foF2 ≈ 2 MHz near 60^{o}CGL may be inferred to go from the

ISIS sub-satellite track (pre-midnight) to the west European (pre-dawn) sector.

December 9, 1971
DMSP pass at 0546 UT, ISIS 2 pass at 0612 UT,
K_p = 3- →1o, AE = 119→50

The auroral activity in the midnight sector during this period has been well-documented by air-borne all sky camera photographs [Whalen et al, 1977]. The DMSP and ISIS-2 observations comprising this event were made during a quiet interval between two substorms that differed greatly in their magnetic and ionospheric signatures [Whalen et al, 1977]. Figure 4.5 reproduces the DMSP image with an overlay of geographic co-ordinates projected to 100 km altitude. Figure 4.6 is a composite representation, in corrected geomagnetic co-ordinates, of the equatorward edge of the diffuse aurora, topside sounder foF2 values along the ISIS-2 track, and ground-based foF2 data and TEC observations from the network of stations depicted in Figure 4.3. The foot of the poleward wall of the trough appears 6.3^{o} lower in latitude than the equatorward edge of the diffuse (DMSP) aurora. Along the ISIS sub-satellite track (which in this case falls within the DMSP field of view) the separation between the top of the poleward wall and the auroral boundary is found to be 3.3^{o}. The ionosonde stations immediately to the east show foF2≃ 5MHz to the north of ϕ_a and foF2 ≃ 2 MHz equatorward of ϕ_{pw}. Looking further to the east, ionosondes poleward of ϕ_a give foF2 in the 5-6 MHz, again typical of poleward wall values, while sites equatorward of ϕ_{pw} show foF2 values more typical of the trough minimum (i.e., foF2 ≃ 2-3 MHz). The trough in TEC has its

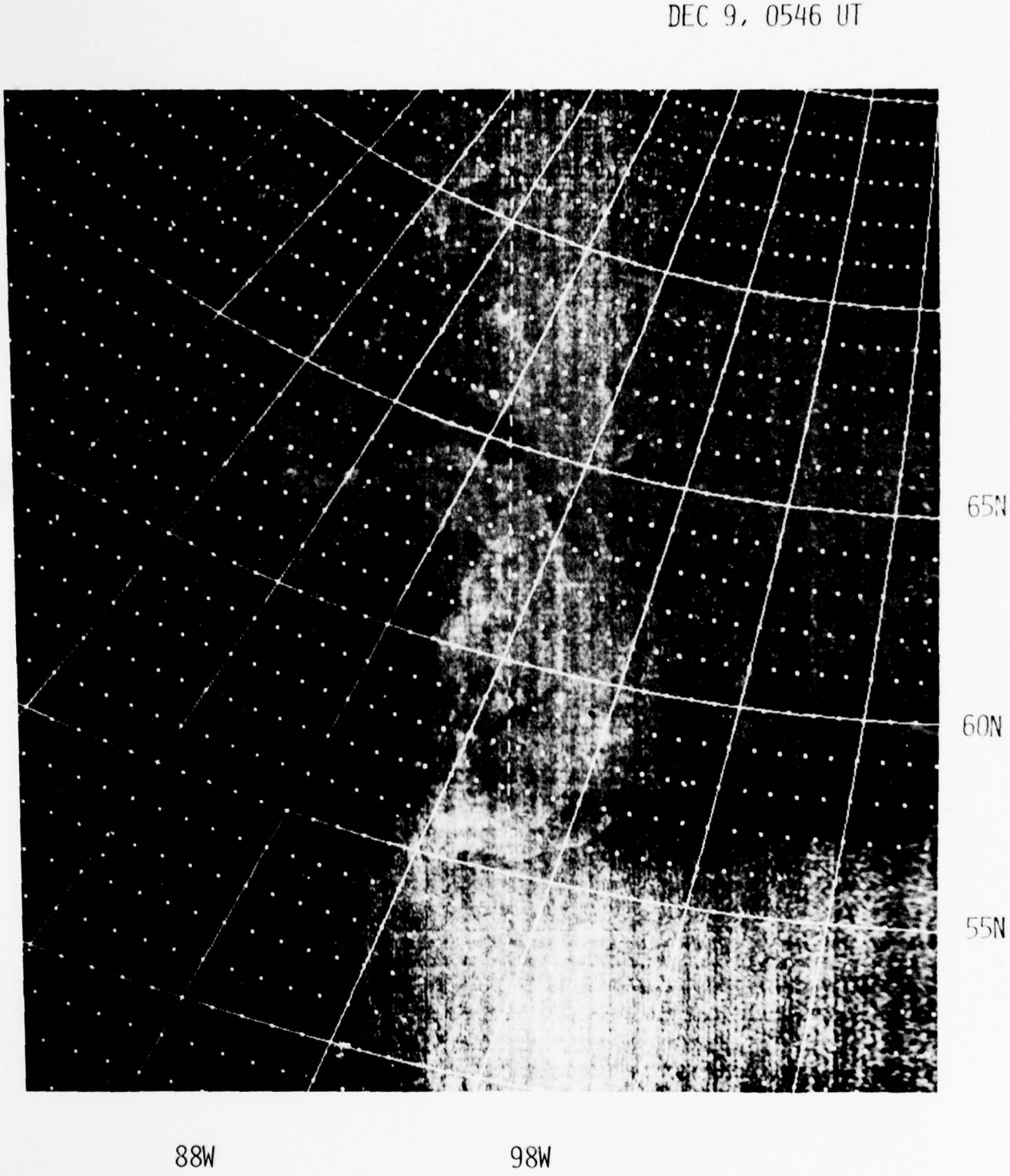

FIGURE 4.5 DMSP image of part of the night side auroral region in the northern hemisphere recorded about 0546 UT on December 9, 1971. Geographic coordinates (100 km) are overlaid.

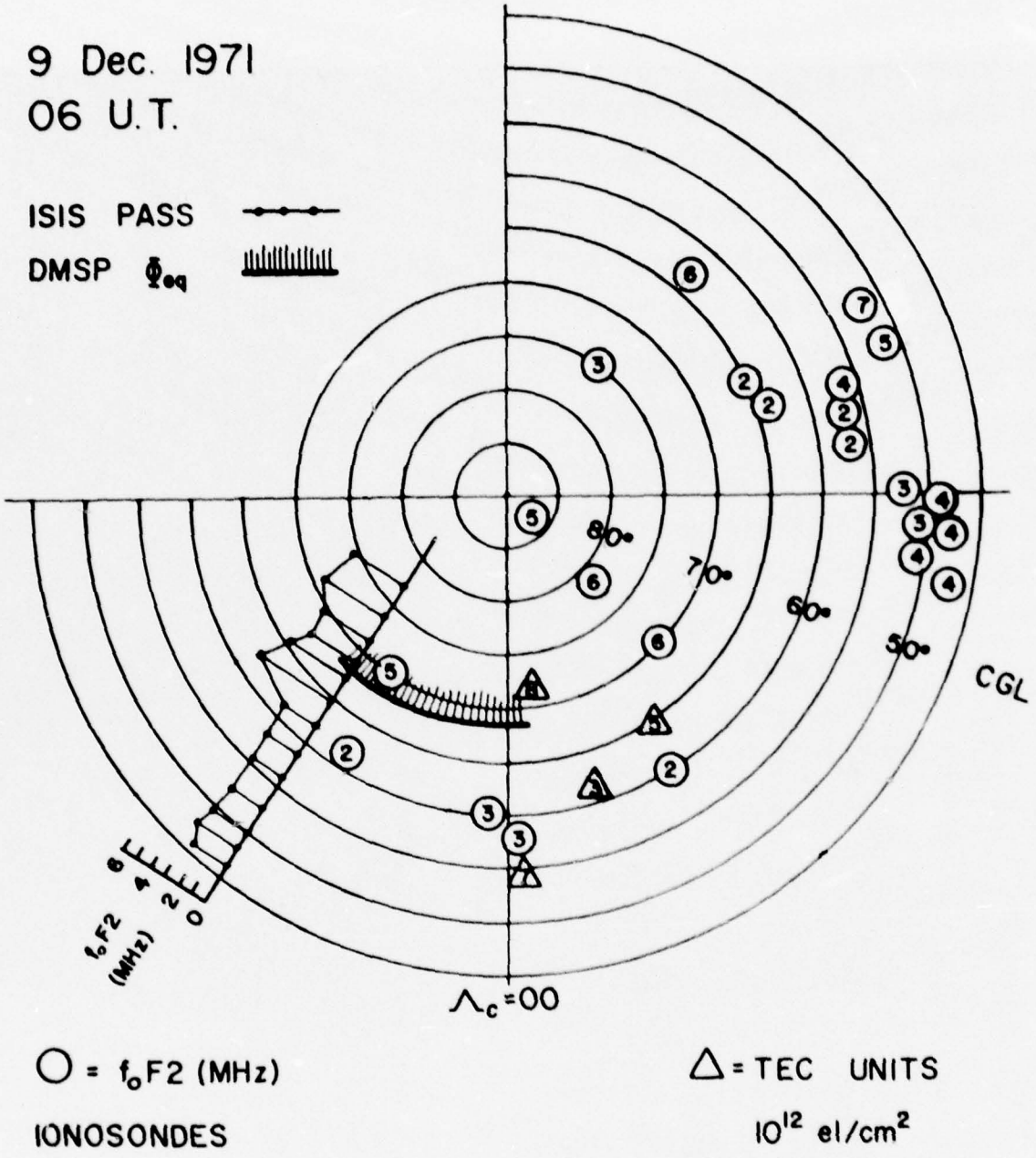

FIGURE 4.6 North polar view in CGL showing the location of near-simultaneous ISIS and DMSP satellite data for 0600 UT on 9 December 1971. Ground-based foF2 values and TEC data at 0600 UT from the network shown in Figure 4.3 are presented using integer values.

minimum near 60^{o}, with 3×10^{12} el/cm^2 consistent with a 2 MHz peak. In fixing the trough minimum at ≈2 MHz near 60^{o}, no inconsistency is found within the DMSP field of view, and indeed as far to the east as the western European foF2 stations in the predawn sector.

The history of the continuous (∿ diffuse) aurora in the 0000-1200 UT period on December 9, 1971 has been documented by Whalen et al, [1977]. They find rapid and extensive latitudinal motions of both the equatorward and poleward boundaries of the continuous aurora --an observation somewhat at odds with the relative stability of diffuse auroras advanced in earlier studies [Lui and Anger, 1973; Akasofu, 1974]. Note that the differences between the 'diffuse' aurora (ISIS-2 scanning photometer) and the diffuse auroral emissions seen on the DMSP images (4,500 - 11,000 Å) may be more significant than commonly assumed.

December 11, 1971: Two sets of consecutive passes
DMSP pass at 0655 UT, ISIS 2 pass at 0725 UT, $K_p = 0$, AE = 32 → 29; DMSP pass at 0837 UT, ISIS 2 pass at 0917 UT, $K_p = 0 \rightarrow 1$, AE = 23 → 38.

Figures 4.7 and 4.8, together with Figures 4.9 and 4.10, represent two sets of DMSP/ISIS data from successive passes during an interval of very minor and apparently localized magnetic activity. Very faint suggestions of magnetic disturbance seen at ∿ 0930 UT at College and Fort Churchill occur ∿ 13 minutes after the second of the satellites (ISIS 2) has traversed the night side auroral latitudes. While the two sets of satellite observations may be broadly categorized as quiet-time findings, it is also

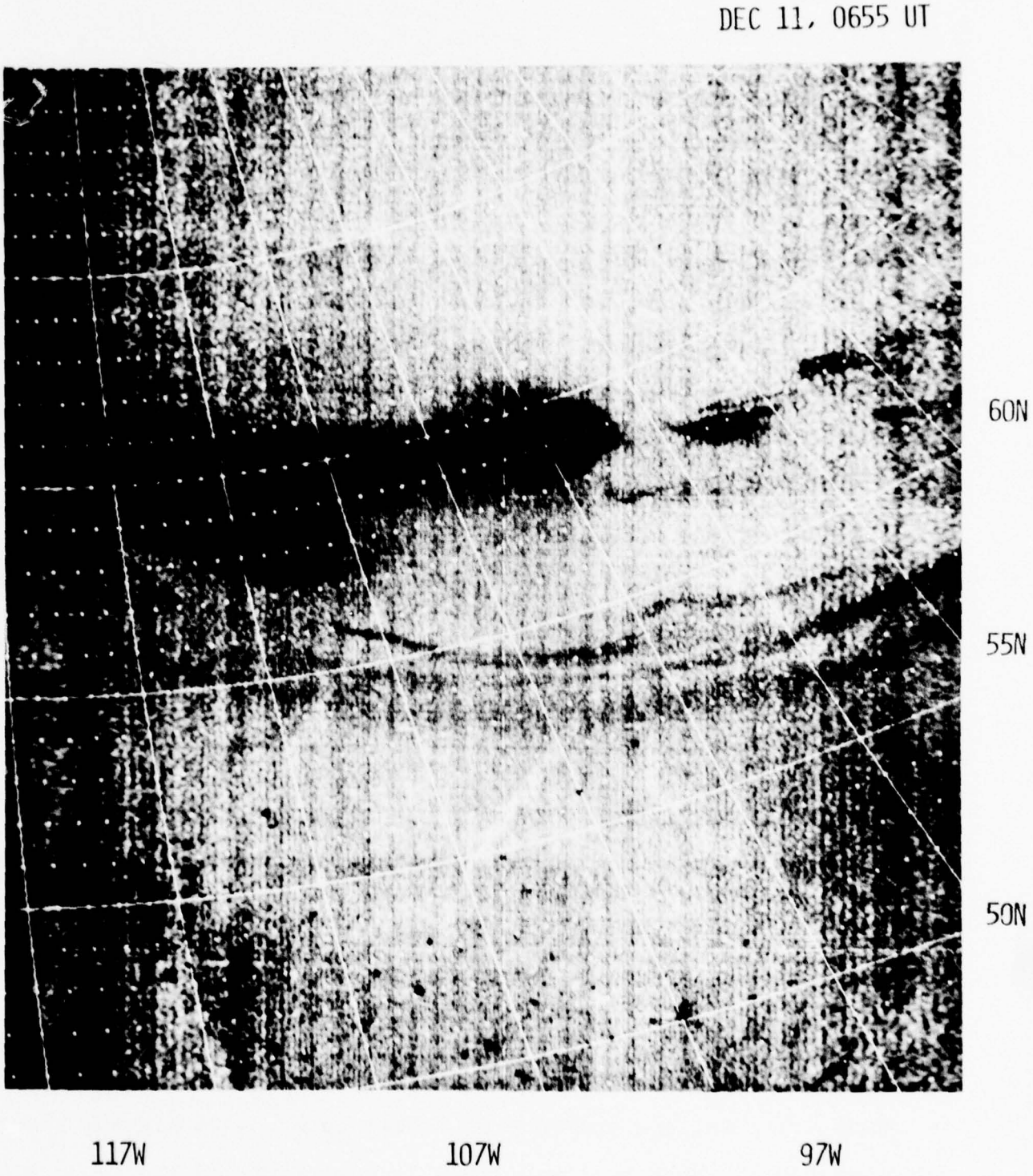

FIGURE 4.7 DMSP image of part of the night side auroral region in the northern hemisphere recorded about 0655 UT on December 11, 1971. Geographic coordinates (100 km) are overlaid.

clear that magnetic activity was slowly on the ascendancy during the UT interval under consideration. The response of the equatorward edge of the diffuse aurora to increasing magnetic activity in this instance appears to be a significant poleward migration: from 67.0°CGL (0655 UT) to 69.2°CGL (0837 UT). It is also interesting to note that as the equatorward auroral boundary moves poleward, so does the poleward wall of the trough, and by about the same amount (See table 4.1).

The trough and its poleward wall are not as well defined in these two instances as they were in the December 9 and 21 cases. Table 4.1 summarizes the trough features at the ISIS longitudes, and Figures 4.8 and 4.10 present "instantaneous" composite plots of the DMSP/ISIS/ground-based observations. Using a worst-case approach, the poleward walls may be located at (61.6 - 63.8)°CGL during the 0725 UT pass and at (63.5 - 66.2)°CGL during the 0917 UT pass. Correspondingly, the equatorward edges of the diffuse aurora (ϕ_a) are (5.4 to 3.2) degrees and (5.7 to 3.0) degrees respectively, poleward of the trough's poleward wall.

In both cases, the ISIS pass occurred to the west of the DMSP image. At 7 UT (Fig 4.8), a trough minimum with foF2 < 2 MHz near 60°CGL at the satellite track, and a poleward wall with foF2 ≃ 3 MHz, appears to be a consistent feature as monitored by the ionospheric stations within and to the east of the DMSP field of view. In figure 4.10, the 9 UT case shows a remarkable consistency between the trough characteristics to the west and east of

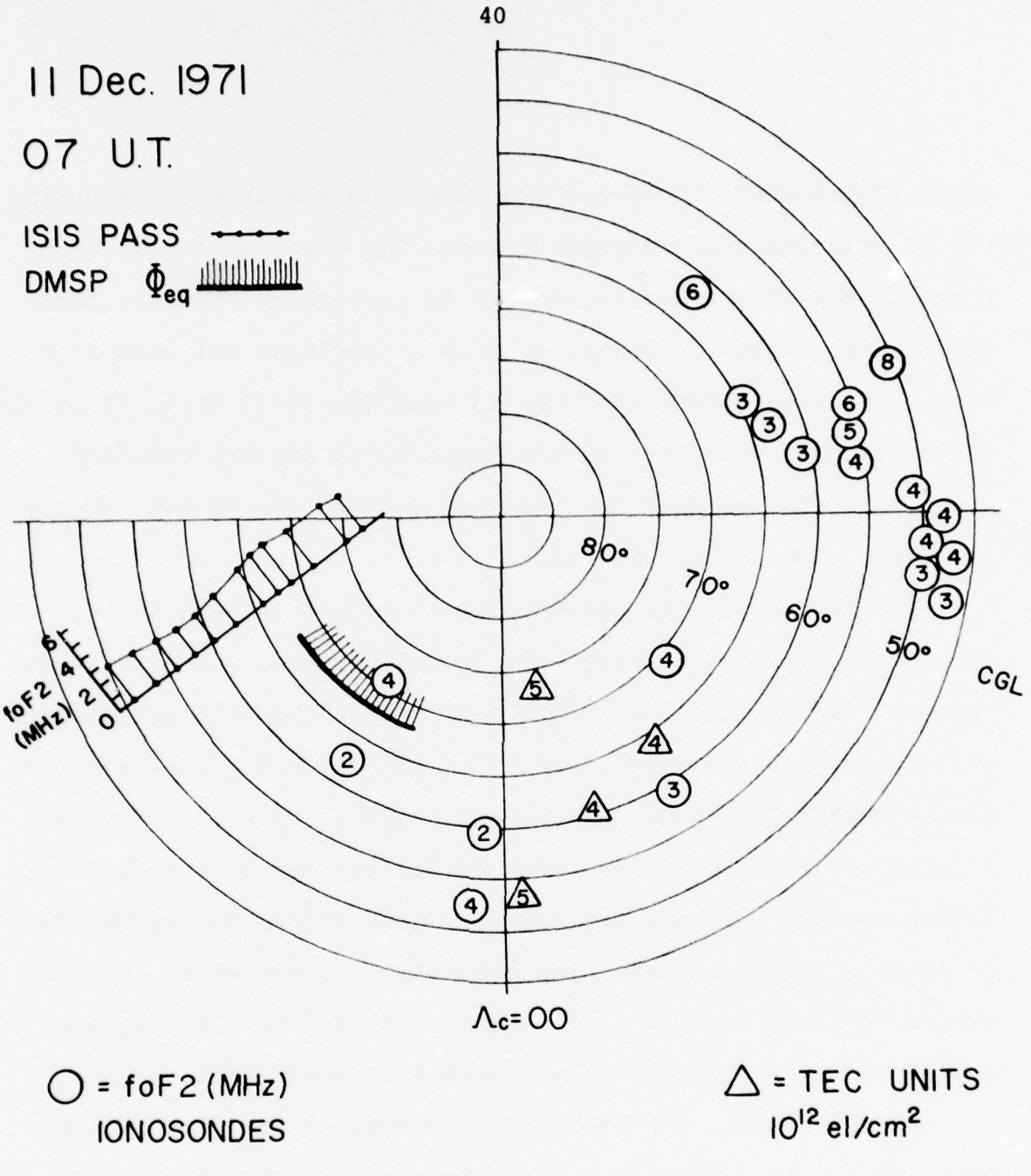

FIGURE 4.8 North polar view in CGL showing the location of near-simultaneous ISIS and DMSP satellite data for 0700 UT on 11 December 1971. Ground-based foF2 values and TEC data at 0700 UT from the network shown in Figure 4.3 are presented using integer values.

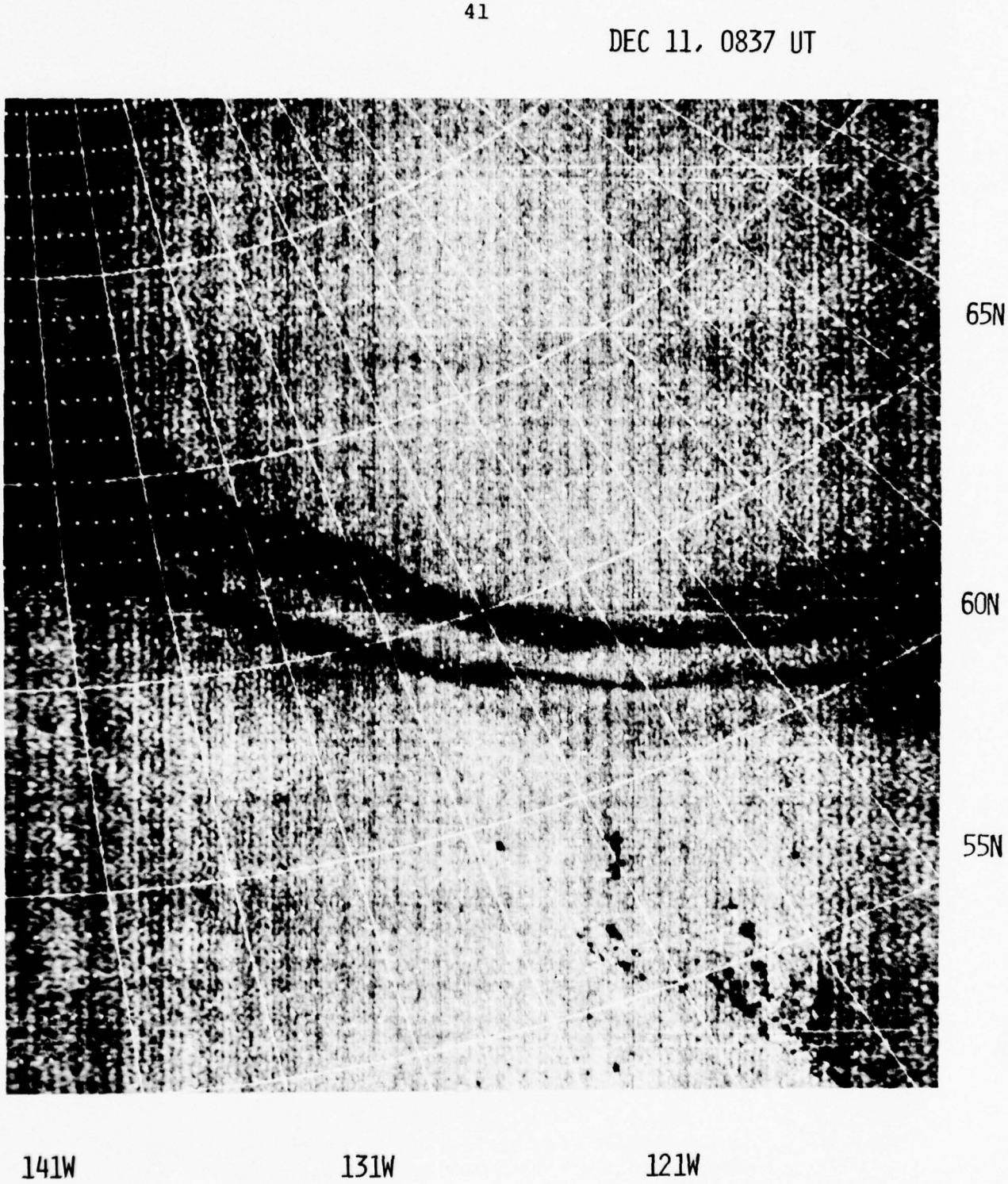

FIGURE 4.9 DMSP image of part of the night side auroral region in the northern hemisphere recorded about 0837 UT on December 11, 1971. Geographic coordinates (100 km) are overlaid.

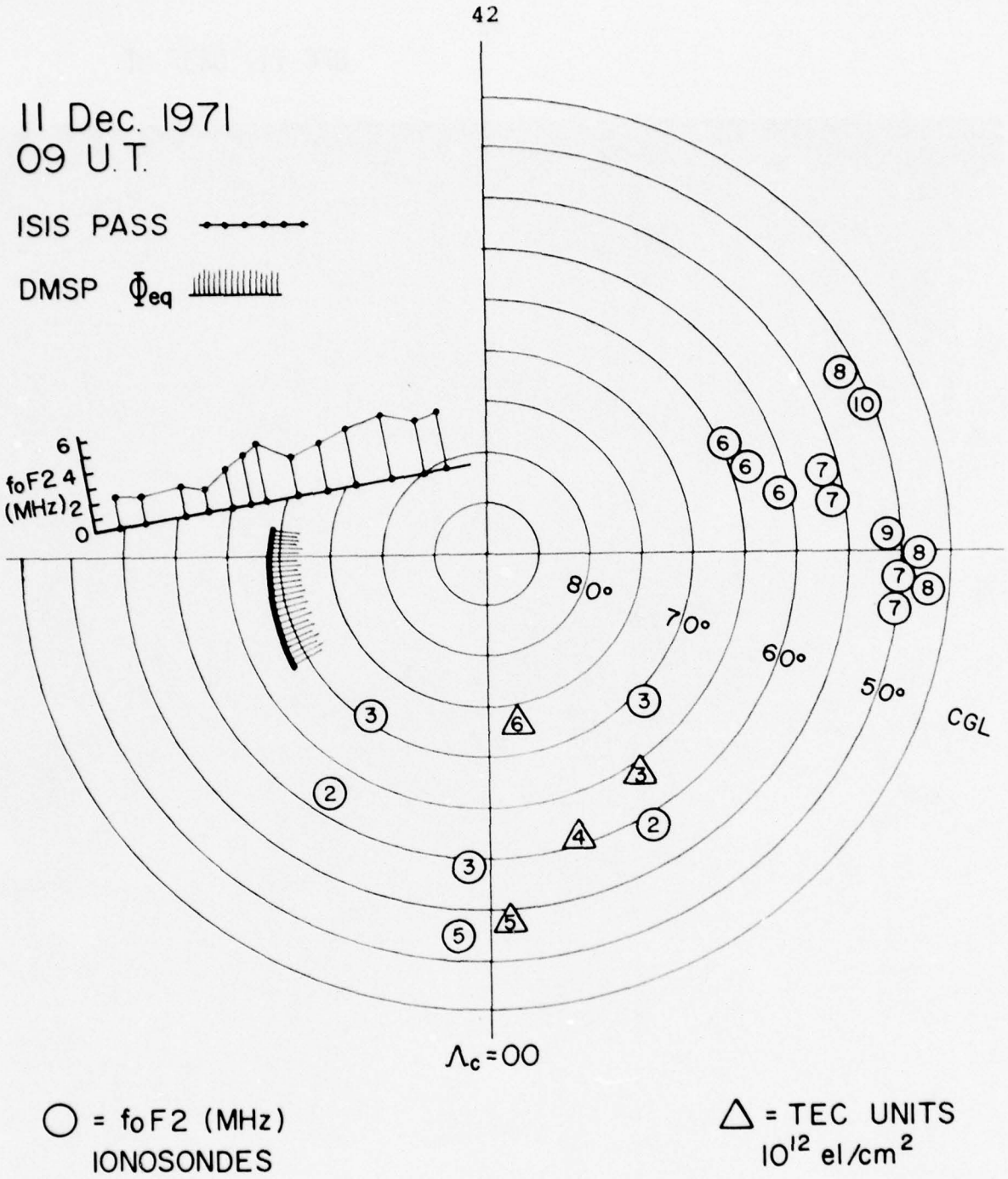

FIGURE 4.10 North polar view in CGL showing the location of near-simultaneous ISIS and DMSP satellite data for 0900 UT on December 11, 1971. Ground-based foF2 values and TEC data at 0900 UT from the network shown in Figure 4.3 are presented using integer values.

the DMSP photo. The TEC observations from Thule and Narssarssuaq, coupled to the foF2 values from Narssarssuaq and St. Johns, support a poleward wall near 70^{o}CGL from the midnight to dawn sector.

DISCUSSION

On the basis of ten events investigated in this study, the equatorward edge of the diffuse aurora seen on the DMSP images is not colocated with the poleward wall of the main electron density trough. Apart from the observation that the auroral boundary (DMSP) is always found poleward of the trough boundary, no systematic relationship between $\Delta\phi$ and magnetic activity (K_p or AE, for example) could be found. Of course a much larger statistical sample than contained in the limited number of case studies used here is needed to establish whether or not a systematic behavior, does indeed exist.

The spectral range of the DMSP detector spans the 4,500 Å - 11,000 Å range, with maximum sensitivity at ∿8,000 Å; this is not well-suited for auroral investigations although approximate proportionality between the visible and DMSP range is believed to exist [Pike and Whalen 1974]. The diffuse glow seen in the DMSP images may contain contributions not only from the diffuse aurora [Lui and Anger, 1973; Whalen et al, 1971; Snyder et al, 1974] but from D-region auroral absorption, unresolved discrete auroras, F-layer auroras and ground albedo [Whalen et al, 1977]. It is not possible at this stage to establish detailed physical correspondences between the auroral displays on the DMSP images and particle precipitations and hence between the optical images and the particle-generated electron density gradients. Bates et al [1973] have reported several observations of the electron density maximum

associated with the poleward wall occurring 1 to 2 degrees equatorward of the visual aurora. The equatorward transport of aurorally produced plasma may be induced by equatorward neutral winds, as Bates et al suggests or by $\underline{E} \times \underline{B}$ drifts--the latter effect presumably being present to varying extents at all times.

By far the major portion of the ionization produced by precipitating particles in the auroral energy range is located below the F-region peak [Rees 1963; Banks et al, 1974; Mantas and Walker, 1976] and chemical processes rather than vertical diffusion dominate the evolution of particle-generated ionization. The main trough is customarily characterized at and above the F-region peak where in-situ production of ionization by soft ($\simeq$ a few hundred eV) particles maximizes. The particles responsible for much of the auroral emissions have a harder (1-20 keV) spectrum. The diffuse aurora seen on the DMSP images and the poleward wall of the main electron density trough are probably generated by different classes of precipitating particle populations.

The time-scales involved in auroral emissions and F-region electron density changes are vastly different. While precipitation, excitation and emission are more-or-less concurrent processes, accumulation of ionization needs at least a few tens of minutes to grow to appreciable magnitudes in the auroral ionosphere [Chacko and Mendillo, 1977; Whitekker 1977]. Transient precipitation events (those that are not steady in time and space for at least a few tens of minutes) could therefore lead to auroral emissions to be captured on the DMSP images without an

accompanying enhancement of electron densities at h_{max} and above.

Figure 4.11 illustrates schematically the problem of establishing correspondences among particle precipitations, auroral emissions and electron densities in the topside ionosphere. In addition to chemical reactions, vertical diffusion, heating, $\underline{E}$-fields and neutral winds also influence the redistribution of auroral ionization. Estimates of the strengths of these complex processes in the auroral ionosphere should contribute to an explanation of the apparent lack of spatial correlation observed between DMSP images and topside electron density features.

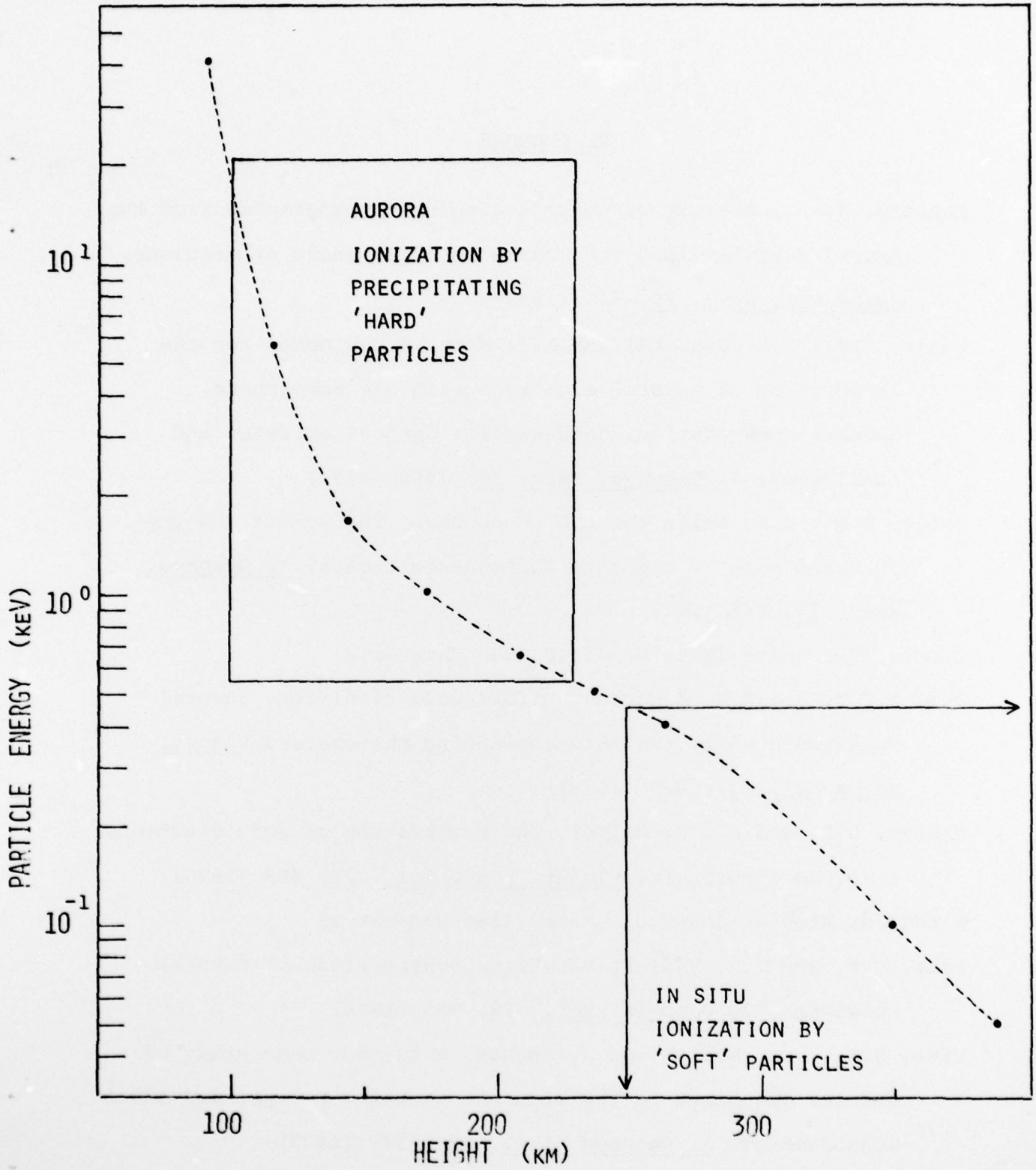

FIGURE 4.11 The altitude of maximum ion production as a function of the energy of precipitating electrons. Data taken from Rees (1963) and Mantas and Walker (1976).

REFERENCES

Akasofu, S.-I., A study of auroral displays photographed from the DMSP-2 satellite and the Alaska meridian chain of stations, Space Sci. Rev., 16, 617 (1974).

Banks, P.M., C.R. Chappell and A.F. Nagy, A new model for the interaction of auroral electrons with the atmosphere: spectral degradation, backscatter, optical emission and ionization, J. Geophys. Res., 79, 1459 (1974)

Bates, H.F., A.E. Belon and R.D. Hunsucker, The aurora and the poleward edge of the main ionospheric trough, J. Geophys. Res., 78, 648 (1973)

Chacko, C.C. and Michael Mendillo (See Chapter 3)

Lui, A.T.Y. and C.D. Anger, A uniform belt of diffuse auroral emission seen by the ISIS 2 scanning photometer, Planet. Space Sci., 21, 809 (1973)

Mantas, G.P. and J.C.G. Walker, The penetration of soft electrons into the ionosphere, Planet. Space Sci., 24, 409 (1976)

Mendillo, Michael and C.C. Chacko (See Chapter 2)

Pike, C.P. and J.A. Whalen, Satellite observations of auroral substorms, J. Geophys. Res., 79, 985 (1974)

Pike, C.P., J.A. Whalen and J. Buchau, A 12-hour case study of auroral phenomena in the midnight sector: F-layer and 6300Å measurements, J. Geophys. Res., 82, 3547 (1977)

Rees, M.H., Auroral ionization and excitation by incident energetic electrons, Planet. Space Sci., 11, 1209 (1963)

Snyder, A.L., S.-I. Akasofu and T.N. Davis, Auroral substorms observed from above the north polar region by a satellite, J. Geophys. Res., 1393 (1974)

Weber, E.J., J.A. Whalen, R.A. Wagner and J. Buchau, A 12-hour case study of auroral phenomena in the midnight sector: Electrojet and precipitating particle characteristics, J. Geophys. Res., 82, 3557 (1977)

Whalen, J.A., J. Buchau and R.A. Wagner, Airborne ionospheric and optical measurements of noontime aurora, J. Atmos. Terr. Phys., 33, 661 (1971)

Whalen, J.A., R.A. Wagner and J. Buchau, A 12-hour case study of auroral phenomena in the midnight sector: oval, polar cap and continuous auroras, J. Geophys. Res., 82, 3529 (1977)

Whitekker, J.H., The transient response of the topside ionosphere to precipitation, Planet. Space Sci., 25, 773 (1977)

APPENDIX A: h_{max}

There appears to exist a substantial lack of consistent observational information regarding the latitudinal variation of h_{max} from mid- to high latitudes. There are, however, a few individual stations at which the local time variation of h_{max} has been examined closely [e.g. Thomas and Robbins, 1958]. Coordinated observations along a closely-spaced meridian chain of stations should, in principle, yield data describing the latitudinal variation of h_{max}. However, on account of the large number of parameters on which h_{max} is known to depend (LT, solar zenith angle, solar cycle, season, neutral winds, magnetic activity-heating, E-fields, auroral ionization) observations spanning the entire range of each of these variables are needed to construct average profiles of h_{max} as a function of latitude. No such comprehensive set of observations seems to be available in the existing literature.

Figure A-1 shows the latitudinal variation of h_{max} between 40^{o} and 80^{o} CGL for the "base-level" conditions described in Chapters 2 and 3. In examining this figure, one should note that (1) the number of observations on the dayside is much smaller than that on the nightside, (2) the derived values of h_{max} are generally considered to be less reliable than the N_{max} values obtained from foF2 scalings and (3) the observations were made by a topside sounder which usually locates h_{max} up to a few tens of km higher than a bottomside sounder.

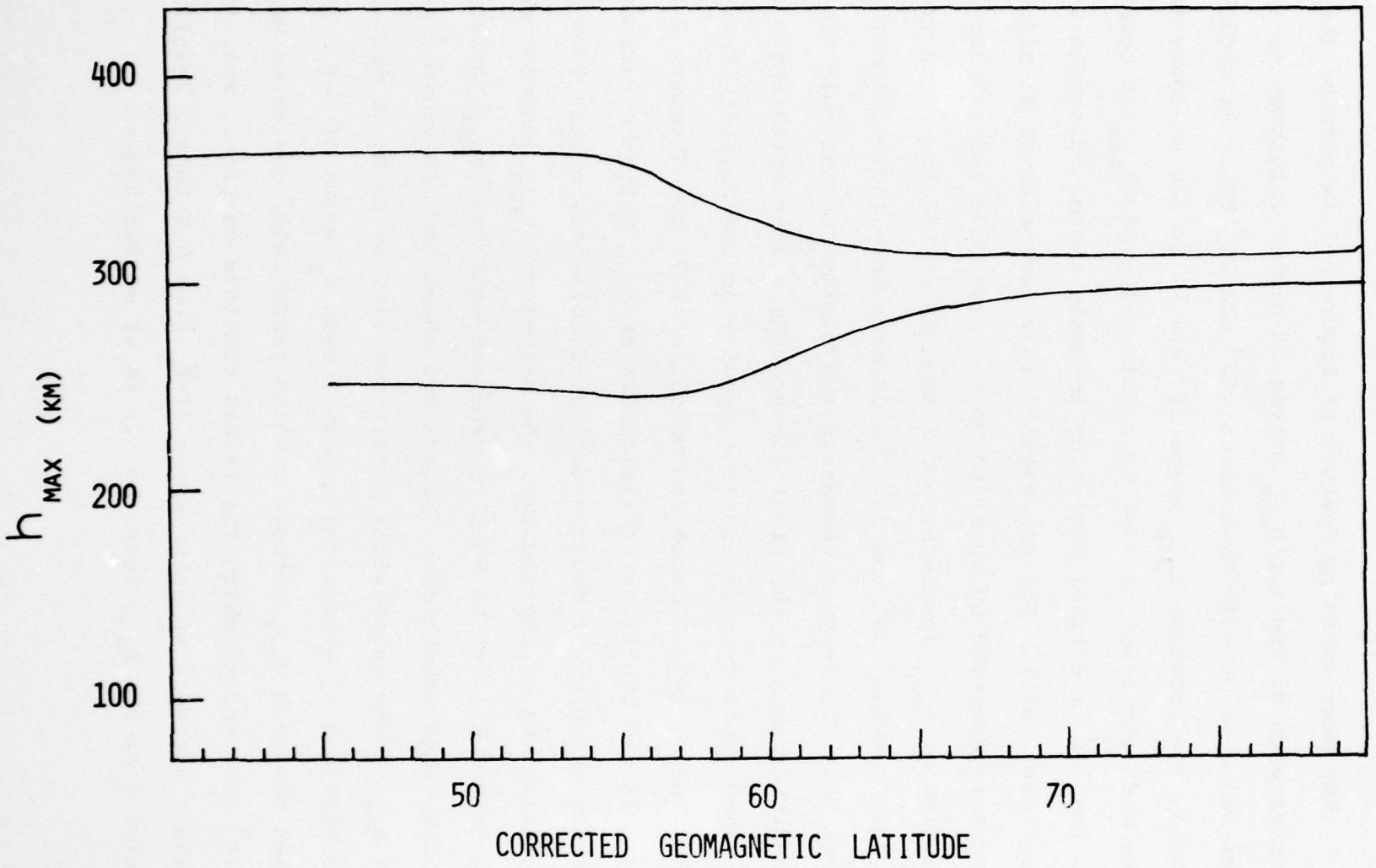

FIGURE A.1 Variation of h_{max} with latitude near noon (lower curve) and near midnight (upper curve) during quiet ($Kp \leq 1+$) conditions.

The most striking feature of Figure A-1 is perhaps the near-convergence of the two h_{max} curves at higher latitudes to a common value of 300-310 km between $\sim 67^{o}$ and 80^{o} CGL. At midlatitudes, the noontime h_{max} value of $\sim$250 km is 110 km lower than the midnight level of $\sim$360 km. This value of Δh_{max} is comparable to the 100 km diurnal variation commonly quoted (Rishbeth and Garriott, 1969). The convergence to a common level at high latitudes is achieved by lowering on the nightside and raising on the dayside of h_{max} levels by equal amounts of $\sim$50 km. This transition occurs between $\sim 55^{o}$ and 65^{o} CGL at both noon and midnight. Note that this CGL range encompasses the minimum of the main electron density trough on the nightside and the solar-zenith-angle controlled rapid drop in electron density on the dayside [Mendillo and Chacko, 1977; Chacko and Mendillo 1977; see Chapters 2 and 3].

If the functional relationship of h_{max} with the various variables on which it depends can be established, either from model calculations or empirically, the base-level h_{max} behavior shown in Figure A-1 can be used to generate estimated h_{max} variations under other conditions. Figure A-2 shows the latitudinal behavior of h_{max} under geophysical conditions similar to those pertaining to Figure A-1, except for a higher mean K_p value of 3.5. Note that the noon h_{max} pattern remains essentially unaltered up to $\sim 70^{o}$ CGL, beyond which the values continue to rise. Near midnight, however, an enhancement of $\bar{K}_p$ from 0.5 to 3.5 results in a raising of the h_{max} level by $\sim$20 km at midlatitudes.

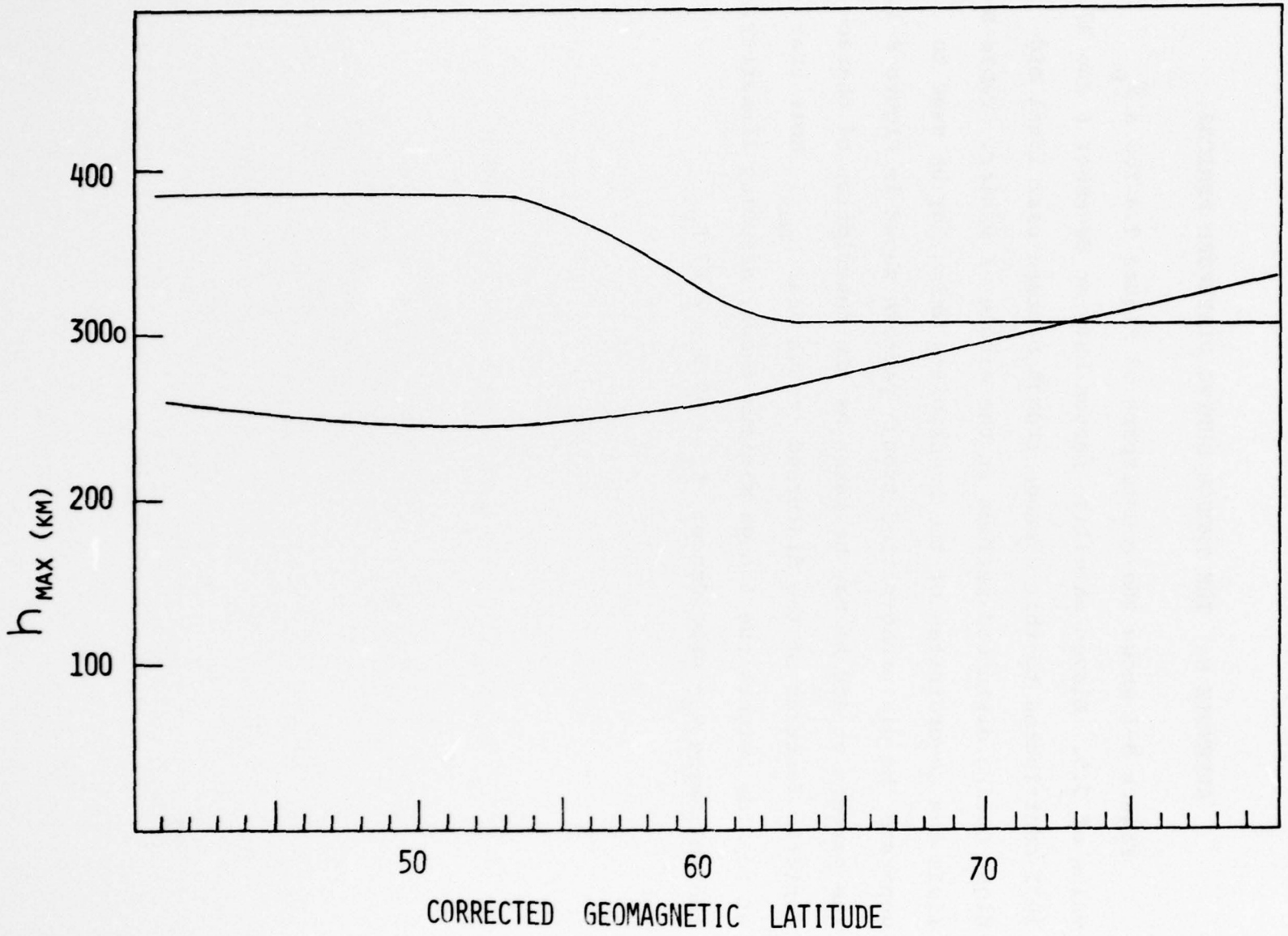

FIGURE A.2 Variation of h_{max} with latitude near noon (lower curve) and near midnight (upper curve) during disturbed (Kp $\geq$ 2-) conditions.

APPENDIX B: THE TROUGH DURING DISTURBED PERIODS.

Figure B-1 shows the counterpart of Figure 2.4 for a $\bar{K}_p$ value of 3.5. Eleven satellite passes between December 6 and 27, 1971 contributed to this average trough pattern near local midnight during disturbed periods in the middle of winter. Table B-1 lists the co-ordinates of the breakpoints which may be used to generate the disturbed-period trough pattern shown in Figure B-1. The pattern at 450 km may be taken as the description of characteristic features of the disturbed trough near h_{max}. Note that at topside heights the trough minimum shows, assuming linearity, the following K_p- dependence: $\Lambda_T = 60.5 - 1.67\ K_p$.

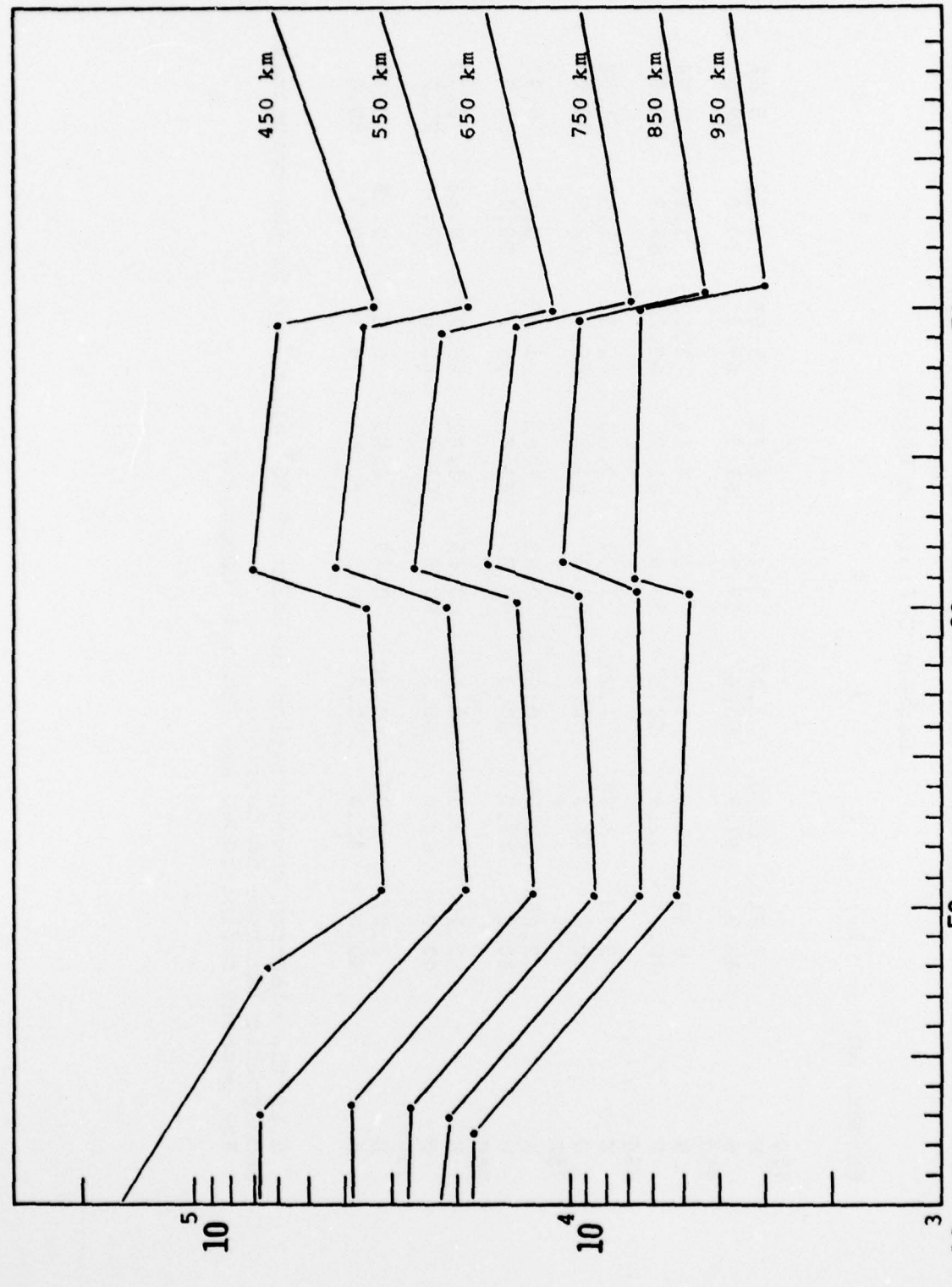

FIGURE B.1 A representation for disturbed trough constructed using 11 ISIS 2 passes in December 1971.

TABLE B-1. Coordinates of Ne(h) Versus Latitude Segments from Parameterization Analysis of $K_p \geq 2-$ Troughs

Height, km	Segment Definition Points							
	1	2	3	4	5	6	7	8
450								
N	7.01	6.30	3.07	3.43	6.96	5.85	3.27	5.61
Θ	40.0	47.9	50.6	59.9	61.2	69.4	70.0	80.0
550								
N	6.59	6.58	1.85	2.12	4.15	3.53	1.82	2.96
Θ	40.0	42.9	50.5	59.9	61.2	69.2	69.9	80.0
650								
N	3.73	3.76	1.21	1.37	2.55	2.17	1.07	1.58
Θ	40.0	43.3	50.4	60.1	61.3	69.1	69.9	80.0
750								
N	2.65	2.60	0.84	0.92	1.61	1.37	0.66	0.92
Θ	40.0	43.2	50.3	60.3	61.4	69.3	70.1	80.0
850								
N	2.15	2.06	0.64	0.65	1.02	0.91	0.43	0.57
Θ	40.0	42.8	50.3	60.6	61.4	69.6	70.3	80.0
950								
N	1.87	1.77	0.50	0.47	0.63	0.63	0.29	0.38
Θ	40.0	42.4	50.2	60.3	60.9	70.1	70.7	80.0

N is the electron concentration in units of 10^4 el/cm^3; Θ is the corrected geomagnetic latitude in degrees.

For segment definitions, see Table 1, Chapter 2.

REFERENCES

Rishbeth, H. and O.K. Garriott, Introduction to Ionospheric Physics, p 171, Academic Press, New York, 1969.

Thomas, J.O. and A. Robbins, The electron distribution in the ionosphere over Slough-II, Disturbed days, J. Atmos. Terr. Phys., 13, 131 (1958).